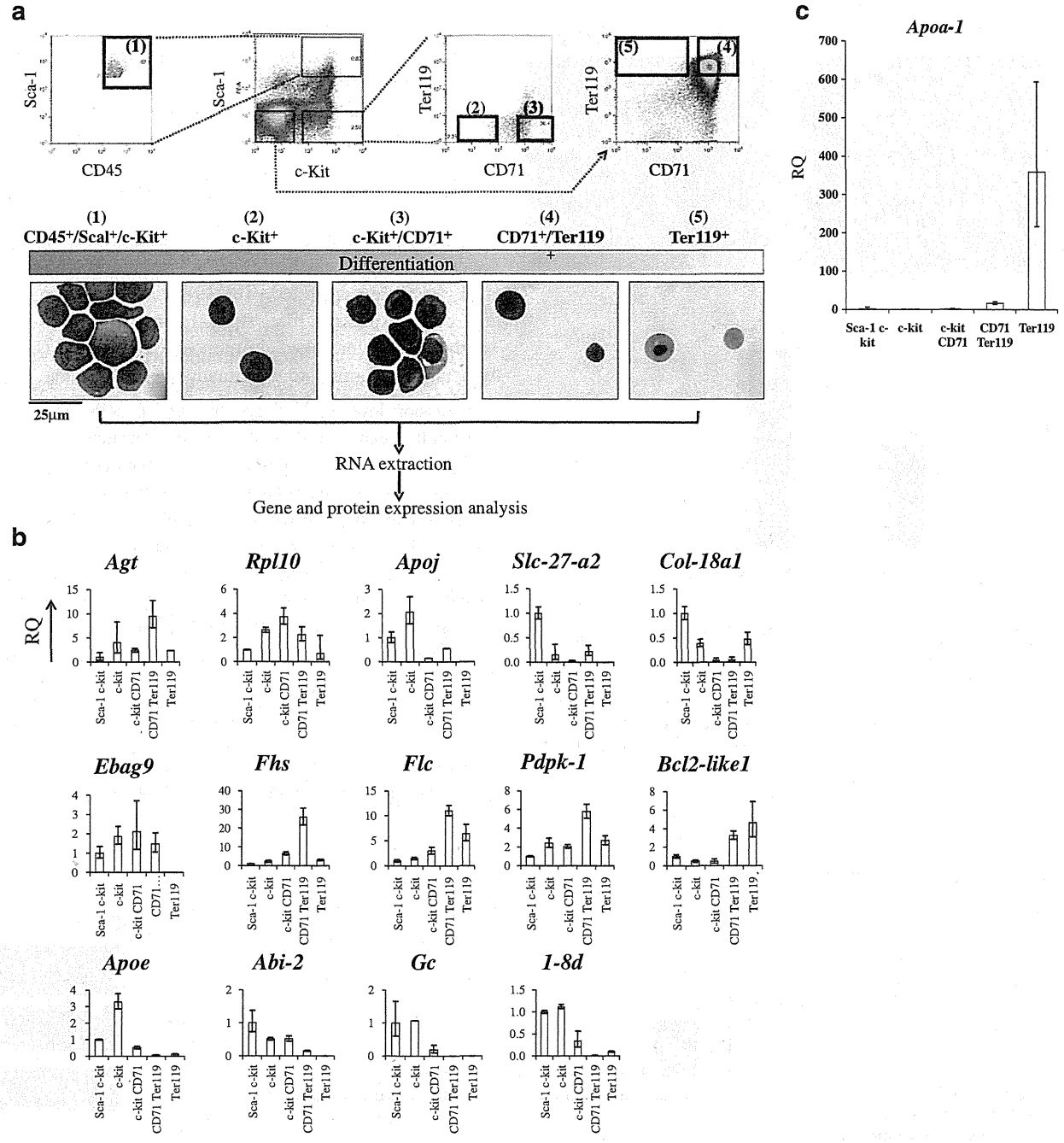

Fig. 3 Isolation of maturing erythroid populations from mouse FL cells. **a** Hematopoietic stem cells and maturing erythroid populations were isolated from 12.5 dpc mouse FL based on the expression of the surface markers CD45 (common leukocyte antigen), Sca-1 (stem cell antigen-1), c-Kit (stem cell factor receptor), CD71 (transferrin receptor) and Ter119 (Glycophorin A-associated antigen). The cytospins of each cellular fraction were prepared for May-Grunwald-Giemsa staining. As erythroid cells mature, the cell size decreased and finally the erythrocytes were enucleated. **b** mRNA expression patterns of candidate genes during erythroid cell maturation. The mRNA levels of candidate genes in maturing erythroid populations were analyzed by qRT-PCR. Total RNA was isolated from FL cells of 12.5 dpc embryos (Bars represent the means ± SD). The horizontal axes indicate the HSC fraction and the erythroid cell stage. Erythroid cell development proceeds from left to right. The vertical axes indicate the relative quantitation (RQ) of mRNA expression with the Sca-1$^+$/c-Kit$^+$ cell fraction set at an RQ value of 1. **c** The expression of mouse *Apoa-1* was significantly increased in the terminal maturation stages (Ter119$^+$ cell fraction) of cells obtained from 12.5 dpc FL

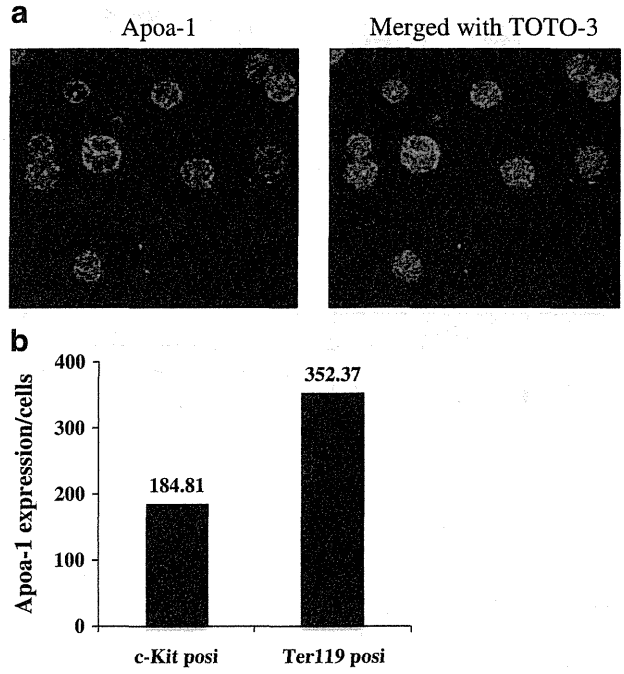

Fig. 4 Apoa-1 protein expression in mouse FL cells. **a** Immunohistochemistry. Ter119-positive cells from 12.5 dpc FL cells were cytospun and stained with an anti-mouse Apoa-1 antibody. Apoa-1-positive cells (*red*) were observed in 12.5 dpc FL cells. Nuclei were stained with TOTO3 (*blue*). **b** ELISA. c-Kit-positive cells and Ter119-positive cells from 12.5 dpc FL cells were sorted. Protein was extracted from each fraction and then analyzed by a sandwich ELISA. The expression levels of the mouse Apoa-1 proteins are shown for each fraction

Ter119-positive mature erythrocytes (Fig. 3c). The mRNA levels of *Apoa-1* increased approximately 350-fold, respectively, in the Ter119-positive cell population compared to the HSC population, suggesting that both of these genes are involved in the terminal maturation of erythroid cells.

Expression of the Apoa-1 Protein in Mouse FL Cells

To determine whether Apoa-1 is expressed at the protein level in mouse erythroid cells, immunohistochemical analyses were performed. Ter119-positive cells in mouse FL cells expressed the Apoa-1 protein (Fig. 4a). A sandwich enzyme-liked immunosorbent assay (ELISA) was also performed to quantitatively analyze the protein expression level in 12.5 dpc mouse FL cells. Because it is difficult to extract sufficient amounts of protein for an ELISA from individually fractionated cells in the populations shown in Fig. 3a, we compared the following two groups to analyze protein expression: c-Kit-positive cells, namely ((1)+(2)+(3) in Fig. 3) and Ter119-positive cells or ((4)+(5) in Fig. 3). As shown in Fig. 4b, Apoa-1 protein expression was approximately two-fold higher in Ter119-positive cells than c-Kit-positive cells, indicating that Apoa-1 expression correlates with terminal erythroid maturation at the protein level.

APOA-1 Expression in Human Peripheral Blood

To determine whether APOA-1 is useful as a terminal erythroid marker in human samples, we examined mRNA

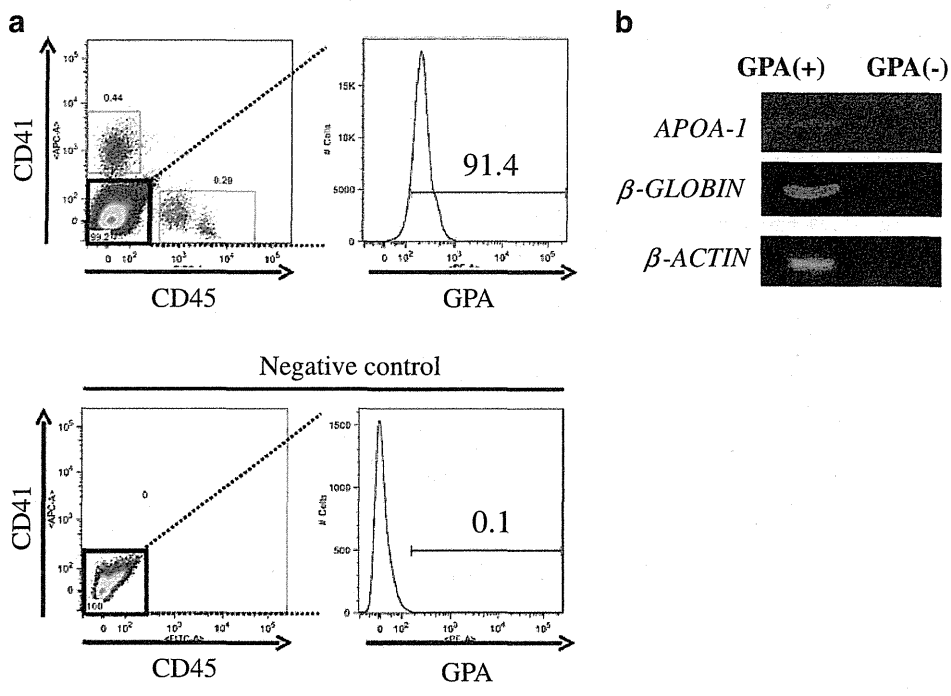

Fig. 5 *APOA-1* gene expression in human peripheral blood. **a** Erythrocytes and reticulocytes were isolated from human peripheral blood based on the expression of surface markers CD41 (integrin IIb), CD45 (common leukocyte antigen) and GPA (glycophorin A). **b** RT-PCR was performed to assess expression of human *APOA-1*. Human *β-GLOBIN* expression was analyzed to confirm that erythrocytes and reticulocytes had been isolated by flowcytometry. *APOA-1* was expressed in human peripheral blood

expression in human peripheral blood (PB) erythrocytes and reticulocytes. Erythrocytes and reticulocytes were isolated from peripheral blood by flow cytometry based on the expression of the cell surface markers glycophorin A (GPA), CD41 and CD45. In the PB, 91.4% of the CD41-/CD45-cells were positive for GPA (Fig. 5a). Reverse transcriptase PCR (RT-PCR) analysis showed that *β-GLOBIN* was expressed in GPA-positive cells, indicating that erythrocyte and reticulocyte mRNA was successfully extracted from the PB (Fig. 5b). Furthermore, *APOA-1* mRNA was expressed in the same fraction, demonstrating that this molecules can be used as a potential marker for terminal erythroid maturation in humans as well as mice.

Discussion

The goal of this study was to identify novel genes that are expressed during the terminal, EPO-independent maturation of erythroid cells. A two-step approach consisting of a lentiviral human FL cDNA library screen followed by an analysis of the gene expression patterns during erythropoiesis was performed to efficiently identify target genes.

This strategy had two clear advantages. First, it is important to establish a screening system that can detect erythropoiesis-related genes in an EPO-independent manner. A human FL cDNA library can be screened to identify novel genes. In this study, UT-7/EPO cells were transduced with a FL cDNA expression lentiviral library to detect genes that generate erythroid colonies in semi-solid medium in the absence of the EPO signaling pathway. Second, this screen could examine the effects of a large number (6×10^5) of genes on erythroid maturation. As humans are estimated to have approximately $2–3\times10^4$ genes, our screening encompassed a sufficient number of human cDNAs.

BCL2-like1 (BCL2L1) was one of the candidate genes identified in the first screen. *BCL2L1* encodes an anti-apoptotic protein that plays an important role in erythropoiesis in the absence of EPO [16]. Therefore, the results of our first screen strongly indicated that this system could be used to identify EPO-independent erythropoiesis-related genes. Other candidate genes included *FHS* and *FLC*, which encode iron-binding proteins, and *APOE, APOA-1*, *APOJ* and *SLC27A2,* which encode lipid metabolism-related proteins. Both iron and lipid metabolism are important cellular processes that regulate erythroid maturation [17–19]. We also identified a number of genes that were not previously implicated in erythropoiesis, including a vitamin D-binding protein (*GC*), vasoregulator (*AGT*), estrogen-responsive gene (*EBAG9*), collagen type 18 (*COL18A1*), ribosomal protein (*RPL10*) and several kinase-related proteins (*PDPK1* and *ABI-2*).

We also specifically identified a gene that was upregulated in the terminal stages of erythrocyte maturation. The identification of this gene is significant because very few molecular markers can be used to examine this stage of erythropoiesis. The candidate gene, *APOA-1*, was particularly interesting. APOA-1 is a major protein component of high-density lipoprotein (HDL) in the plasma and promotes the efflux of cholesterol from the tissues to the liver for excretion [20]. APOA-1 is a cofactor for lecithin cholesterol acyltransferase (LCAT), which is responsible for the formation of most plasma cholesteryl esters.

APOA-1 interacts with the ATP-binding cassette transporter ABCA1 (member 1 of human transporter sub-family ABCA) [21]. A recent report demonstrated that the APOA-1/ABCA1 pathway functions as an anti-inflammatory receptor by activating Janus Kinase 2 (JAK2)/Signal Transducers and Activation of Transcription3 (STAT3) in macrophages [22]. JAK2/STAT3 and/or JAK2/STAT5 are central signal pathways in erythroid cells [23]. Therefore, APOA-1/ABCA1 may activate the JAK2/STAT3 and/or JAK2/STAT5 pathway during the terminal maturation of erythroid cells.

It is intriguing to note that defects in APOA-1 are associated with low HDL levels observed in HDL deficiency type 1, which includes analphalipoproteinemia or Tangier disease. In Tangier disease patients, APOA-1 fails to associate with HDL. This inability to bind HDL is likely due to the faulty conversion of pro-APOA-1 molecules into mature chains, either due to a defect in the converting enzyme or a specific structural defect [24–26]. Furthermore, red blood cells in patients with Tangier disease have stomatocytosis and hemolytic anemia [27]. Moreover, patients with beta-thalassemia major as well as sickle cell disease have lower levels of APOA-1 in their plasma than healthy controls [28]. This abnormal erythrocyte morphology could be partially explained by a recent report by Holm TM et al., which showed that knockout mice with defects in the high-density lipoprotein receptor SR-BI have abnormal erythrocyte morphology. On the other hand, the fractional catabolic rate (FCR) for APOA-1 was significantly increased in patients with myeloproliferative disorders, including polycythemia vera, compared with healthy controls [29]. Therefore, accelerated red blood cell production could be also supported by increased APOA-1 catabolism. Further studies including both in vitro and/or in vivo analyses of APOA-1 knockouts are necessary to demonstrate the direct importance of APOA-1 in the maturation of red blood cells.

This study is the first to report that APOA-1 is a novel molecular marker for terminal erythroid maturation from HSC. In combination with Ter119 antigen or glycophorin A antigen, this molecule can potentially be used to identify mature erythrocytes in in vitro cultured erythroid cell

sources such as ES or iPS cells. It will be necessary to further investigate whether APOA-1 plays pivotal roles in erythroid cell maturation and is a useful maturation marker.

Acknowledgements The authors would like to thank Chiyo Mizuochi, Yuka Horio, Tatsuya Sasaki and Michiko Ushijima at Kyushu University for excellent technical assistance. This work was supported by a grant from the Project for Realization of Regenerative Medicine from the Ministry of Education, Culture, Sports, Science and Technology and by a grant from the BASIS project from the Ministry of Education, Culture, Sports, Science and Technology. T. Inoue is supported by research fellowships from the Japan Society for the Promotion of Science for Young Scientists.

Disclosures The authors indicate no potential conflicts of interest.

References

1. Weissman, I. L. (2000). Stem cells: units of development, units of regeneration, and units in evolution. *Cell, 100*, 157–168.
2. Mikkola, H. K., & Orkin, S. H. (2006). The journey of developing hematopoietic stem cells. *Development, 133*, 3733–3744.
3. Medvinsky, A., & Dzierzak, E. (1996). Definitive hematopoiesis is autonomously initiated by the AGM region. *Cell, 86*, 897–906.
4. Sugiyama, D., & Tsuji, K. (2006). Definitive hematopoiesis from endothelial cells in the mouse embryo; a simple guide. *Trends in Cardiovascular Medicine, 16*, 45–49.
5. Ema, H., & Nakauchi, H. (2000). Expansion of hematopoietic stem cells in the developing liver of a mouse embryo. *Blood, 95*, 2284–2288.
6. Palis, J. (2008). Ontogeny of erythropoiesis. *Current Opinion in Hematology, 15*, 155–161.
7. McGrath, K., & Palis, J. (2008). Ontogeny of erythropoiesis in the mammalian embryo. *Current Topics in Developmental Biology, 82*, 1–22.
8. Hiroyama, T., Miharada, K., Sudo, K., Danjo, I., Aoki, N., & Nakamura, Y. (2008). Establishment of mouse embryonic stem cell-derived erythroid progenitor cell lines able to produce functional red blood cells. *PLos One, 3*, e1544.
9. Kina, T., Ikuta, K., Takayama, E., et al. (2000). The monoclonal antibody TER-119 recognizes a molecule associated with glycophorin A and specifically marks the late stages of murine erythroid lineage. *British Journal Haematology, 109*, 280–287.
10. Zhang, J., Socolovsky, M., Gross, A. W., & Lodish, H. F. (2003). Role of Ras signaling in erythroid differentiation of mouse fetal liver cells: functional analysis by a flow cytometry-based novel culture system. *Blood, 102*, 3938–3946.
11. Kurita, R., Sasaki, E., Yokoo, T., et al. (2006). Tal1/Scl gene transduction using a lentiviral vector stimulates highly efficient hematopoietic cell differentiation from common marmoset (Callithrix jacchus) embryonic stem cells. *Stem Cells, 24*, 2014–2022.
12. Kurita, R., Oikawa, T., Okada, M., et al. (2008). Construction of a high-performance human fetal liver-derived lentiviral cDNA library. *Molecular and Cellular Biochemistry, 319*, 181–187.
13. Komatsu, N., Yamamoto, M., Fujita, H., et al. (1993). Establishment and characterization of an erythropoietin-dependent subline, UT-7/Epo, derived from human leukemia cell line, UT-7. *Blood, 82*, 456–464.
14. Suzuki, N., Suwabe, N., Ohneda, O., et al. (2003). Identification and characterization of 2 types of erythroid progenitors that express GATA-1 at distinct levels. *Blood, 102*, 3575–3583.
15. Walkley, C. R., & Orkin, S. H. (2006). Rb is dispensable for self-renewal and multilineage differentiation of adult hematopoietic stem cells. *Proceedings of the National Academy of Sciences of the United States of America, 103*, 9057–9062.
16. Dolznig, H., Habermann, B., Stangl, K., et al. (2002). Apoptosis protection by the Epo target Bcl-X(L) allows factor-independent differentiation of primary erythroblasts. *Current Biology, 12*, 1076–1085.
17. Gelvan, D., Fibach, E., Meyron-Holtz, E. G., & Konijn, A. M. (1996). Ferritin uptake by human erythroid precursors is a regulated iron uptake pathway. *Blood, 88*, 3200–3207.
18. Meyron-Holtz, E. G., Vaisman, B., Cabantchik, Z. I., et al. (1999). Regulation of intracellular iron metabolism in human erythroid precursors by internalized extracellular ferritin. *Blood, 94*, 3205–3211.
19. Holm, T. M., Braun, A., Trigatti, B. L., et al. (2002). Failure of red blood cell maturation in mice with defects in the high-density lipoprotein receptor SR-BI. *Blood, 99*, 1817–1824.
20. Breslow, J. L., Ross, D., McPherson, J., et al. (1982). Isolation and characterization of cDNA clones for human apolipoprotein A-I. *Proceedings of the National Academy of Sciences of the United States of America, 79*, 6861–6865.
21. Fitzgerald, M. L., Morris, A. L., Rhee, J. S., Andersson, L. P., Mendez, A. J., & Freeman, M. W. (2002). Naturally occurring mutations in the largest extracellular loops of ABCA1 can disrupt its direct interaction with apolipoprotein A-I. *Journal of Biological Chemistry, 277*, 33178–33187.
22. Tang, C., Liu, Y., Kessler, P. S., Vaughan, A. M., & Oram, J. F. (2009). The macrophage cholesterol exporter ABCA1 functions as an anti-inflammatory receptor. *Journal of Biological Chemistry, 47*, 32336–32343.
23. Richmond, T. D., Chohan, M., & Barber, D. L. (2005). Turning cells red: signal transduction mediated by erythropoietin. *Trends in Cell Biology, 15*, 146–155.
24. Zannis, V. I., Lees, A. M., Lees, R. S., & Breslow, J. L. (1982). Abnormal apoprotein A-I isoprotein composition in patients with Tangier disease. *Journal of Biological Chemistry, 257*, 4978–4986.
25. Gordon, J. I., Sims, H. F., Lentz, S. R., Edelstein, C., Scanu, A. M., & Strauss, A. W. (1983). Proteolytic processing of human preproapolipoprotein A-I. A proposed defect in the conversion of pro A-I to A-I in Tangier's disease. *Journal of Biological Chemistry, 258*, 4037–4044.
26. Schmitz, G., Assmann, G., Rall, S. C., Jr., & Mahley, R. W. (1983). Tangier disease: defective recombination of a specific Tangier apolipoprotein A-I isoform (pro-apo A-i) with high density lipoproteins. *Proceedings of the National Academy of Sciences of the United States of America, 80*, 6081–6085.
27. Reinhart, W. H., Gossi, U., Butikofer, P., et al. (1989). Haemolytic anaemia in analpha-lipoproteinaemia (Tangier disease): morphological, biochemical, and biophysical properties of the red blood cell. *British Journal Haematology, 72*, 272–277.
28. Sasaki, J., Waterman, M. R., & Cottam, G. L. (1986). Decreased apolipoprotein A-I and B content in plasma of individuals with sickle cell anemia. *Clinical Chemistry, 32*, 226–227.
29. Ginsberg, H. N., Le, N. A., & Gilbert, H. S. (1986). Altered high density lipoprotein metabolism in patients with myeloproliferative disorders and hypocholesterolemia. *Metabolism, 35*, 878–882.

CORRIGENDUM

Development 138, 1875 (2011) doi:10.1242/dev.067231

Regulation of hematopoietic cell clusters in the placental niche through SCF/Kit signaling in embryonic mouse

Tatsuya Sasaki*, Chiyo Mizuochi*, Yuka Horio, Kazuki Nakao, Koichi Akashi and Daisuke Sugiyama†

*These authors contributed equally to this work
†Author for correspondence (ds-mons@yb3.so-net.ne.jp)

There was an error published in *Development* **137**, 3941-3952.

The email address of the corresponding author was linked to the incorrect name in the author list. The corrected linking appears above.

The authors apologise to readers for this mistake.

Development 137, 3941-3952 (2010) doi:10.1242/dev.051359

Regulation of hematopoietic cell clusters in the placental niche through SCF/Kit signaling in embryonic mouse

Tatsuya Sasaki[1,*,†], Chiyo Mizuochi[1,†], Yuka Horio[1], Kazuki Nakao[2], Koichi Akashi[3] and Daisuke Sugiyama[1]

SUMMARY

Hematopoietic stem cells (HSCs) emerge from and expand in the mouse placenta at mid-gestation. To determine their compartment of origin and define extrinsic signals governing their commitment to this lineage, we identified hematopoietic cell (HC) clusters in mouse placenta, defined as cells expressing the embryonic HSC markers CD31, CD34 and Kit, by immunohistochemistry. HC clusters were first observed in the placenta at 9.5 days post coitum (dpc). To determine their origin, we tagged the allantoic region with CM-DiI at 8.25 dpc, prior to placenta formation, and cultured embryos in a whole embryo culture (WEC) system. CM-DiI-positive HC clusters were observed 42 hours later. To determine how clusters are extrinsically regulated, we isolated niche cells using laser capture micro-dissection and assayed them for expression of genes encoding hematopoietic cytokines. Among a panel of candidates assayed, only stem cell factor (SCF) was expressed in niche cells. To define niche cells, endothelial and mesenchymal cells were sorted by flow cytometry from dissociated placenta and hematopoietic cytokine gene expression was investigated. The endothelial cell compartment predominantly expressed SCF mRNA and protein. To determine whether SCF/Kit signaling regulates placental HC cluster proliferation, we injected anti-Kit neutralizing antibody into 10.25 dpc embryos and assayed cultured embryos for expression of hematopoietic transcription factors. *Runx1*, *Myb* and *Gata2* were downregulated in the placental HC cluster fraction relative to controls. These observations demonstrate that placental HC clusters originate from the allantois and are regulated by endothelial niche cells through SCF/Kit signaling.

KEY WORDS: Hematopoiesis, Hematopoietic stem cells, Niche, Placenta, SCF/Kit, Mouse

INTRODUCTION

During mouse embryogenesis, hematopoiesis begins in the yolk sac (YS), producing mainly primitive erythroid cells at 7.5 days post coitum (dpc). Shortly thereafter, definitive myelo-erythroid progenitor cells appear in the YS, which seed the fetal liver (Cumano et al., 1996; Ferkowicz and Yoder, 2005; Li et al., 2003; McGrath and Palis, 2005; Palis et al., 1999). This process, termed primitive hematopoiesis, diminishes at 12.5 dpc, when definitive hematopoiesis, which sustains the adult blood system through hematopoietic stem cells (HSCs), begins in fetal liver (Sugiyama and Tsuji, 2006). Although there is controversy over where HSCs are generated – in the extra-embryonic YS or intra-embryonic para-aortic-splanchnopleural mesoderm (P-Sp)/aorta-gonad-mesonephros (AGM) region – recent studies suggest that both the YS and P-Sp/AGM region contain HSCs capable of reconstituting adult bone marrow hematopoiesis (Cumano et al., 1996; Matsuoka et al., 2001; Medvinsky and Dzierzak, 1996; Samokhvalov et al., 2007; Yoder et al., 1997a; Yoder et al., 1997b). Thereafter, these AGM HSCs are thought to circulate and colonize fetal liver, where HSC expansion occurs (Cudennec et al., 1981; Ema and Nakauchi, 2000; Houssaint, 1981; Johnson and Moore, 1975; Sugiyama et al., 2005). In addition to these sites, several reports suggest that the placenta functions not only in gas exchange and fetal nutrition but also in hematopoiesis at approximately mid-gestation (Dancis et al., 1968; Dancis et al., 1977; Melchers, 1979). It is also reported that a significant proportion of hematopoietic progenitor cells (HPCs), including highly proliferative potential colony forming cells (HPP-CFCs), are located in the mouse placenta (Alvarez-Silva et al., 2003). HSCs are detected at this site by 11.5 dpc and the number of long-term reconstituting (LTR)-HSCs dramatically increases from 11.5 dpc to 12.5 dpc, resulting in a 15-fold increase in HSC activity compared with that of the AGM region (Gekas et al., 2005; Ottersbach and Dzierzak, 2005). Taken together, these findings indicate that mouse placenta is likely to be a site for HSC generation and expansion at mid-gestation.

HSCs are regulated by intrinsic programming and by extrinsic signaling from so-called niche cells. However, it is unclear how HSC generation and expansion is regulated in the placenta. To address this issue, we identified hematopoietic cell (HC) clusters, defined as cells expressing embryonic HSC markers such as CD31 (Pecam1 – Mouse Genome Informatics), CD34 and Kit, by immunohistochemistry, enabling us to follow the origin of HC clusters and identify surrounding niche cells. We then used vital dye labeling to demonstrate that HC clusters in placenta originate from the allantois, an embryonic compartment of the placenta. Furthermore, we showed that HC clusters are regulated by vascular niche cells through SCF (Kitl – Mouse Genome Informatics)/Kit signaling.

MATERIALS AND METHODS

Immunohistochemistry

Mouse embryos were dissected out and fixed in 2% paraformaldehyde in PBS, followed by equilibration in 30% sucrose in PBS. Placentas were embedded in OCT compound (SAKURA, Tokyo, Japan) and frozen in liquid nitrogen. Tissues were sliced at 20 μm with a Leica CM1900 UV cryostat, transferred to glass slides (Matsunami, Osaka, Japan) and dried thoroughly. Sections were blocked in 1% BSA in PBS and incubated in

[1]Department of Hematopoietic Stem Cells, SSP Stem Cell Unit, Kyushu University Faculty of Medical Sciences, Fukuoka 812-8582, Japan. [2]Laboratory for Animal Resources and Genetic Engineering Animal Resource Unit, Center for Developmental Biology, RIKEN, Kobe 650-0047, Japan. [3]Department of Medicine and Biosystemic Science, Kyushu University Graduate School of Medical Sciences, Kyushu University, Fukuoka 812-8582, Japan.

*Author for correspondence (ds-mons@yb3.so-net.ne.jp)
†These authors contributed equally to this work

Accepted 21 September 2010

PBS containing 1% BSA with appropriate dilutions of the following primary antibodies: goat anti mouse Kit (1:500; R&D Systems, Minneapolis, MN), rat anti mouse-CD31 (1:500; BD Biosciences, San Diego, CA), rat anti mouse-CD34 (1:500; BD Biosciences), rat anti-mouse CD41 (1:300; BioLegend, San Diego, CA), rat anti-mouse CD45 (1:300; BioLegend) and rat anti-mouse F4/80 (1:300; BioLegend) at 4°C overnight. After washing in PBS three times, sections were incubated with appropriate dilutions of the following secondary antibodies: Alexa Fluor 488 donkey anti-rat IgG (1:300; Invitrogen, Carlsbad, CA) and Alexa Fluor 568 donkey anti-goat IgG (1:300; Invitrogen), as well as TOTO-3 (1:1500; Invitrogen) to stain nuclei, at room temperature for 30 minutes. Samples were mounted on coverslips using fluorescent mounting medium (Dako Corporation, Carpinteria, CA) and were assessed using a FluoView 1000 confocal microscope (Olympus, Tokyo, Japan). Cell aggregates consisting of more than four Kit/CD31 or Kit/CD34 double-positive cells were defined as a hematopoietic cluster.

Cell preparation

Placentas without deciduas and umbilical vessels were used to obtain a single cell suspension. Tissues were passed through 21-gauge needles, incubated with 1 mg/ml collagenase in medium supplemented with 10% fetal bovine serum for 30 minutes at 37°C and filtered through 40 μm nylon cell strainers (BD Biosciences). In analysis and sorting of HSCs, density gradient centrifugation using lymphocyte cell separation medium (Cedarlane Laboratories, Eugene, OR) was performed to harvest mononuclear cells. After centrifugation, the cell pellet was used as the placental cell population.

Flow cytometry and cell sorting

As macrophages are found in HSC preparations (CD31, CD34, Kit), anti-mouse F4/80 antibody was added to identify and to exclude them from analysis. Antibodies used for analysis of the HSC population were: FITC-conjugated anti-mouse CD41 (eBioscience, San Diego, CA), FITC-conjugated anti-mouse Sca-1 (eBioscience), FITC-conjugated anti-mouse EPCR (endothelial protein C receptor) (known as CD201) (Stem Cell Technologies, Vancouver, BC), PE-conjugated anti-mouse CD31 (BD Biosciences), APC-conjugated anti-mouse F4/80 (BioLegend), PE-Cy7-cojugated anti-mouse CD45 (BioLegend), APC-Cy7-conjugated anti-mouse Kit (eBioscience) and Pacific Blue-conjugated anti-mouse CD34 (eBioscience). For endothelial and mesenchymal cell populations, FITC-conjugated anti-mouse Ter-119 (eBioscience), PE-conjugated anti-mouse CD31 (BD Biosciences), APC-conjugated anti-mouse Kit (BD Biosciences), PE-Cy7-cojugated anti-mouse CD45 (BioLegend) and Pacific Blue-conjugated anti-mouse CD34 (eBioscience) were used. Flow cytometric analysis and cell sorting were carried out using a FACS Aria cell sorter (BDIS, San Jose, CA). The data files were analyzed using FlowJo software (Tree Star, San Carlos, CA).

RNA extraction and real-time PCR analysis

Total RNA was isolated using the RNAqueous 4PCR kit (Ambion, Austin, TX). mRNA was reverse transcribed using a High-Capacity RNA-to-cDNA kit (Life Technologies, Carlsbad, CA). The quality of cDNA synthesis was evaluated by amplifying mouse β-actin using PCR. Thirty thermal cycles were used as follows: denaturation at 95°C for 10 seconds, annealing at 60°C for 20 seconds, followed by extension at 72°C for 20 seconds. Gene expression levels were measured by real time-PCR with TaqMan Gene Expression Master Mix and StepOnePlus real-time PCR (Life Technologies). All probes were from TaqMan Gene Expression Assays (Life Technologies). All analyses were performed in triplicate wells; mRNA levels were normalized to β-actin and the relative quantity (RQ) of expression was compared with a reference sample.

Enzyme-linked immunosorbent assay

Proteins were extracted from a flow-sorted endothelial and mesenchymal cell population using a Q Proteome Mammalian Protein Preparation kit (Qiagen, Valencia, CA). SCF in both populations was assayed using an (enzyme-linked immunosorbent assay) ELISA kit (Mouse SCF Immunoassay, R&D Systems), according to the manufacturer's instructions. The optical density was measured in a Thermo Multiskan EX plate reader (Thermo Fisher Scientific, Waltham, MA).

Laser capture micro-dissection

For this procedure, embryos were not fixed and equilibration in sucrose in PBS was not undertaken. Tissues sliced at 20 μm on a cryostat were transferred to glass slides (Matsunami), placed on ice and immediately stored at −80°C until use. After thawing, frozen cryosections were washed in PBS three times and incubated with 1:500 goat anti Kit (R&D Systems) for 60 minutes. After washing in PBS three times, sections were incubated with 1:300 Alexa Fluor 488-conjugated donkey anti-goat IgG (Invitrogen) for 60 minutes to detect Kit-positive cells. In this analysis, fluorescent Kit-positive cell aggregates were considered to be HC clusters, and surrounding cells were marked and cut by laser. Those cells were captured as niche cells and transferred to microcentrifuge tubes containing 10 μl extraction buffer using a Pico Pure RNA Isolation Kit (Molecular Devices, Silicon Valley, CA). Laser capture micro-dissection (LCM) was carried out using an ArcturusXT Laser Capture Microdissection System (Molecular Devices). Immunohistochemistry for LCM was carried out at 4°C, and all solutions were treated with diethylpyrocarbonate (Wako, Osaka, Japan).

CM-DiI labeling of the allantois

CM-DiI (Invitrogen), which binds to the cellular membrane, is non-toxic and remains fluorescent for at least for 4 days, was injected into the basal part of allantois of ICR mouse embryos at 8.25 dpc, prior to chorio-allantoic fusion (Downs and Harmann, 1997). Injected embryos were subjected to whole embryo culture (WEC). Dissection and manipulation of embryos was completed within an hour of starting WEC (Sugiyama et al., 2007).

Intra-cardiac injection

For this procedure, 0.2-0.5 μl of anti-Kit neutralizing antibody (ACK2) (eBioscience) and purified rat IgG2b (isotype control; eBioscience) were administered to ICR mouse embryos at 10.25 dpc, a stage at which we can cut the avascular area of yolk sac with minimal bleeding and inject materials into the heart, by intra-cardiac injection, as previously described (Kulkeaw et al., 2009; Sugiyama et al., 2003). Briefly, embryos in PBS were visualized under a stereomicroscope (Leica Microsystems MZ6, Wetzlar, Germany). Both uterus and deciduo capsularis were removed, and the yolk sac was cut along the yolk sac arteries with care to avoid excessive hemorrhage. The amnion was opened to allow needle access to the heart. The needle was made from glass capillary tubes (Narishige GC-10, Japan) using a micropipette puller (Narishige, Tokyo, Japan). Injected embryos were placed in the WEC system within 1 hour of isolation.

Whole mouse embryo culture (WEC)

Injected embryos were transferred to culture bottles containing rat serum supplemented with 2 mg/ml glucose in a WEC system (Ikemoto Scientific Technology, Tokyo, Japan) and cultured for 6 hours in the case of intra-cardiac injection or 42 hours in the case of CM-DiI labeling at 37°C in the dark with a continuous supply of gas (60% O_2 and 5% CO_2 balanced with N_2) (Kulkeaw et al., 2009; Osumi-Yamashita et al., 1997; Sugiyama et al., 2003; Sugiyama et al., 2005; Sugiyama et al., 2007). After WEC, embryos exhibiting no conspicuous bleeding or anomalies were analyzed.

Mutant strains

Runx1$^{+/-}$ mouse strains were kindly provided by Dr N. Speck. *Evi1*$^{-/-}$ and *Myb*$^{-/-}$ mouse strains were obtained from the Jackson Laboratory (Bar Harbor, ME, USA).

RESULTS

Visualization and characterization of HC clusters in the mouse placenta

Previous studies have identified placental HC clusters primarily by microscopic inspection (Ottersbach and Dzierzak, 2005; Rhodes et al., 2008). To extend these studies, quantify clusters, understand their relationship with other placental components and identify

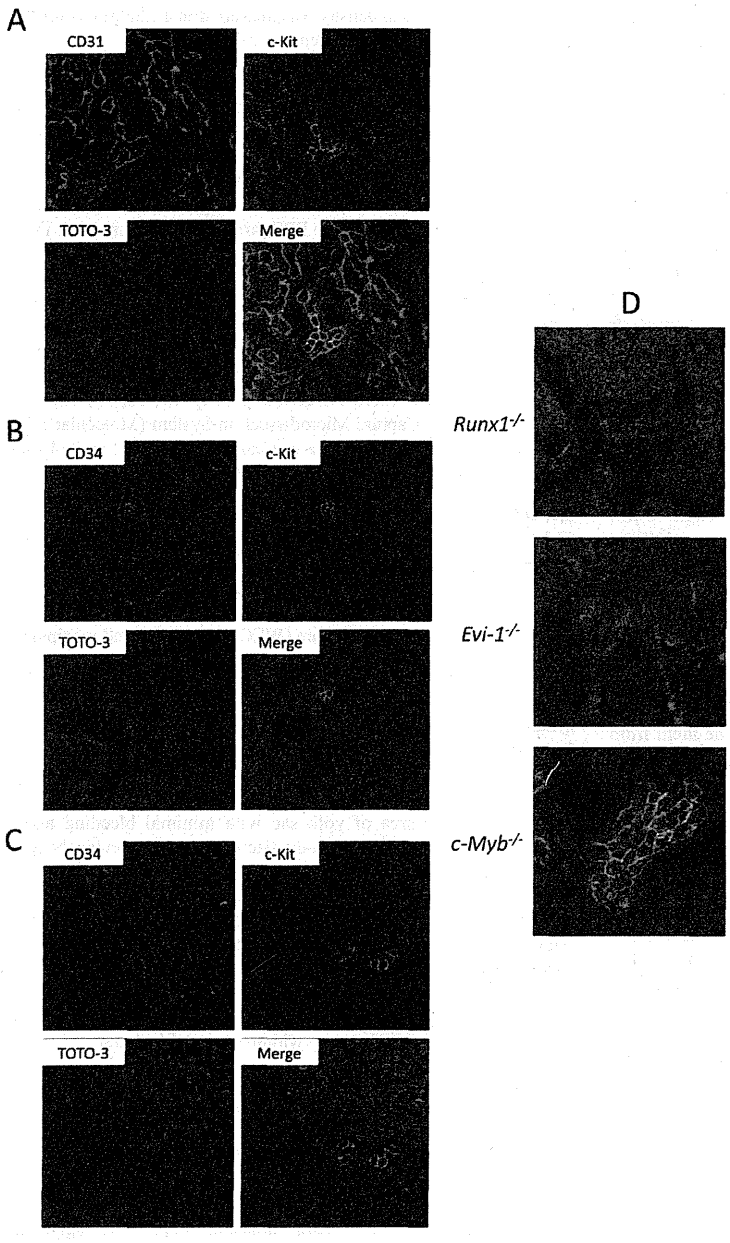

Fig. 1. Confocal images of HC clusters expressing CD31/CD34/Kit in the placenta and aortic region. Sections both of placenta and AGM region were made from ICR mouse embryos at 10.5 dpc, stained with antibodies and observed under confocal microscopy. (**A**,**B**) HC clusters in 10.5 dpc placenta. (A) CD31 (red), Kit (green) and TOTO-3 (blue). (B) CD34 (red), Kit (green) and TOTO-3 (blue). (**C**) HC cluster in the aorta at 10.5 dpc. CD34 (red), Kit (green), and TOTO-3 (blue). (**D**) Altered phenotype of HC clusters in the *Runx1*$^{-/-}$ (upper), *Evi1*$^{-/-}$ (middle) and *Myb*$^{-/-}$ (lower) placentas at 10.5 dpc.

niche cells, we carried out immunohistochemistry using thick (20 μm) cryosections and antibodies recognizing embryonic HSC markers – namely, CD31, CD34 and Kit (Baumann et al., 2004; North et al., 2002; Yoder et al., 1997a). As shown in Fig. 1A,B, using confocal microscopy we defined HC clusters as aggregates of more than four Kit$^+$/CD31$^+$/CD34$^+$ cells. Clusters were attached to the endothelial wall of capillary vessels, the so-called vascular labyrinth region, from 10.5 dpc to 12.5 dpc and were morphologically similar to those seen in the AGM region at 10.5 dpc (Fig. 1C). To further characterize HC clusters, placental tissue was dissociated and analyzed by flow cytometry after first removing macrophages expressing F4/80 (Emr1 – Mouse Genome Informatics). Other HSC markers [such as CD41 (Itga2b – Mouse Genome Informatics), EPCR (Procr – Mouse Genome Informatics; CD201), Sca-1 (Ly6a – Mouse Genome Informatics) and the pan-leukocyte marker CD45 (Ptprc – Mouse Genome Informatics)] were expressed on Kit$^+$/CD31$^+$/CD34$^+$/F4/80$^-$ cells in the placenta (Fig. 2). Among Kit$^+$/CD31$^+$/CD34$^+$/F4/80$^-$ cells, expression of CD41, EPCR (CD201) and Sca-1 decreased from 10.5 dpc to 11.5 dpc, whereas CD45 expression increased over this period. At 12.5 dpc, the embryonic HSC marker CD31 was expressed on 90.2 % of CD34$^+$/Sca-1$^+$/Kit$^+$ cells, which were previously defined as LTR-HSCs (see Fig. S1 in the supplementary material) (Gekas et al., 2005; Ottersbach and Dzierzak, 2005). We next observed HC cluster formation in embryos harboring various mutations associated with aberrant embryonic hematopoiesis (Goyama et al., 2008; Mucenski et al., 1991; North et al., 1999; Okuda et al., 1996; Wang et al., 1996; Yuasa et al., 2005). Specifically, in *Runx1*$^{-/-}$ embryos, no HC clusters were observed inside capillary vessels in the placenta (Fig. 1D, upper). In addition, in *Evi1*$^{-/-}$ (*Mecom*$^{-/-}$ –

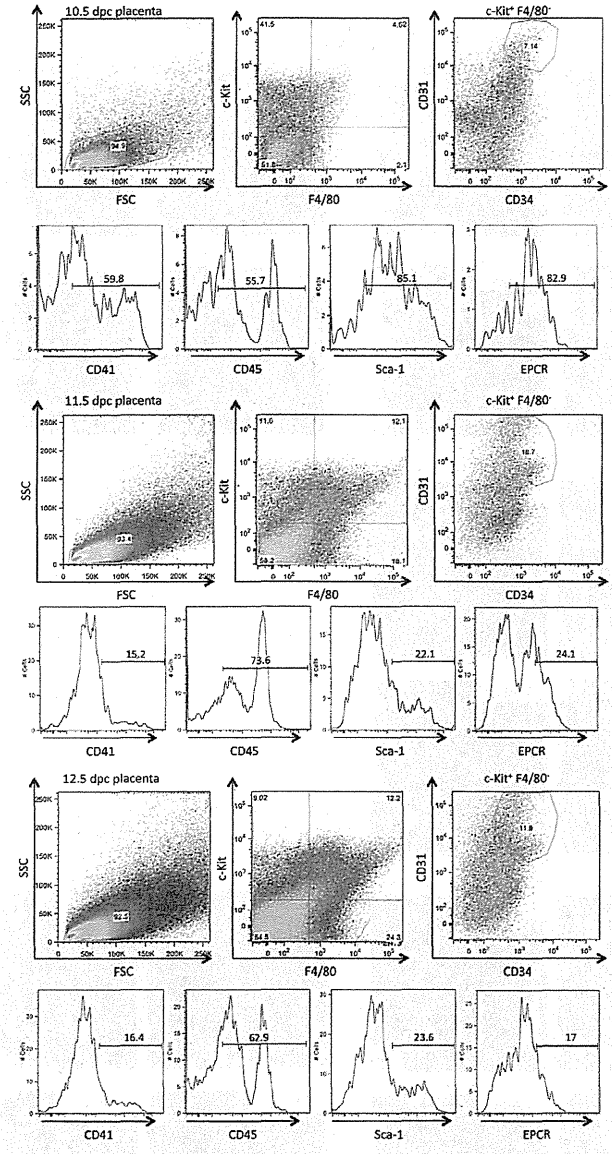

Fig. 2. Flow cytometric analysis of CD31$^+$/CD34$^+$/Kit$^+$/F4/80$^-$ placental cells using surface expression HSC markers. Single cell suspensions of placentas at 10.5, 11.5 and 12.5 dpc, were prepared and analyzed by flow cytometry. The cells that express CD31, CD34 and Kit (markers of HC clusters), but not F4/80 (a macrophage marker) were first gated. Expression of HSC markers, such as CD41, EPCR (CD201), Sca-1 and CD45 was analyzed on CD31$^+$/CD34$^+$/Kit$^+$/F4/80$^-$ cells at 10.5 dpc (upper), 11.5 dpc (middle) and 12.5 dpc (lower).

Mouse Genome Informatics) embryos, no HC clusters were observed inside capillary vessels at the time of abnormal vessel formation (Fig. 1D, middle). Finally, in *Myb*$^{-/-}$ embryos, HC cluster size overall was larger than that seen in wild-type embryos (Fig. 1D, lower).

To further characterize HC clusters, which we define immunohistochemically as cells expressing CD31, CD34 and Kit, we double-stained tissues with CD41, CD45 and F4/80. CD41 marks embryonic HSCs (Mikkola et al., 2003a; Rhodes et al., 2008). HC clusters at 10.5 dpc expressed Kit but not CD41, whereas those at 11.5 dpc expressed both Kit and CD41 (Fig. 3A-C). The intensity of CD41 expression in HC clusters expressing Kit was relatively weak compared with single CD41$^+$ cells. The pan-leukocyte marker CD45 was also weakly expressed HC clusters at the AGM region (Godin and Cumano, 2002). HC clusters at 10.5 dpc expressed Kit but not CD45, whereas those at 11.5 dpc expressed both Kit and CD45 (Fig. 3D,E). Like CD41 expression, the intensity of CD45 expression in HC clusters expressing Kit was relatively weak compared with single CD45$^+$ cells. HC clusters at 10.5 dpc did not express the macrophage marker F4/80 (Fig. 3F). However, circulating Kit$^+$ cells inside blood vessels weakly expressed F4/80 (Fig. 3G,H). It has been reported that F4/80$^+$ macrophages populate the placental mesenchyme (Rhodes et al., 2010). In agreement, we observed some single F4/80$^+$ cells in the mesenchyme, in addition to Kit$^+$/F4/80$^+$ cells in circulation in the placenta (data not shown). Taken together, our data suggest that by immunohistochemical analysis, combined CD31/CD34/Kit positivity is sufficient to identify HC clusters.

Origin of HC clusters in placenta

To identify the origin of HC clusters in the placenta, we examined them at stages earlier than 10.5 dpc. The allantois, which originates from the embryo, and the extra-embryonic chorion fuse at 8.5 dpc and primary villi begin to develop at 9.0 dpc (Watson and Cross, 2005). HC clusters expressing CD31/CD34/Kit were observed at the allantois and chorionic plate at 9.5 dpc (Fig. 4A). However, HC clusters were not observed in either the allantois or chorion at 8.5 dpc, prior to placenta development (see Fig. S2 in the supplementary material). To follow the fate of allantoic cells, the basal part of the allantois was tagged with CM-DiI at 8.25 dpc and tagged embryos were cultured in a WEC system (Fig. 4B) (Khakoo et al., 2006; Krishnamurthy et al., 2008; Kulkeaw et al., 2009; Osumi-Yamashita et al., 1997; Silva et al., 2006; Sugiyama et al., 2003). After 42 hours in culture, all embryos developed normally (data not shown). The allantois fused to the chorion, forming both the umbilical cord and placenta, in which CM-DiI fluorescence could be detected (n=4) (Fig. 4C). Sections of embryos tagged with CM-DiI were stained for Kit by immunohistochemistry. CM-DiI/Kit-positive HC clusters were observed in the developing placenta, strongly suggesting that these clusters are derived from the allantois (Fig. 4D,E; see Fig. S3 in the supplementary material).

Proliferative status of HC clusters in placenta

Kit$^+$/CD31$^+$/CD34$^+$/F4/80$^-$ cells sorted from placenta at 12.5 dpc exhibited immature morphology, appearing as blast cells when stained with May-Grunwald Giemsa (Fig. 5A). To understand the kinetics of HC cluster formation in placenta from 10.5 dpc to 12.5 dpc, we calculated the number of Kit$^+$/CD31$^+$/CD34$^+$/F4/80$^-$ cells in the placenta at various developmental stages. We observed that the number of Kit$^+$/CD31$^+$/CD34$^+$/F4/80$^-$ cells per placenta increased as the embryo developed (427, 1540 and 3227 cells at 10.5, 11.5 and 12.5 dpc, respectively), suggesting that they are proliferating (Fig. 5B). We next investigated cell cycle status of these cells. Kit$^+$/CD31$^+$/CD34$^+$/F4/80$^-$ cells were flow sorted and stained with an antibody against Ki-67, a marker of cell proliferation (Fig. 5C) (Scholzen and Gerdes, 2000). The proportion of Ki-67$^+$ cells in sorted Kit$^+$/CD31$^+$/CD34$^+$/F4/80$^-$ cells was 80.4%, 77.2% and 48.2% at 10.5, 11.5 and 12.5 dpc, respectively (Fig. 5D), indicating that HC cluster cells in the placenta at 10.5 and 11.5 dpc are more proliferative than cluster cells at 12.5 dpc.

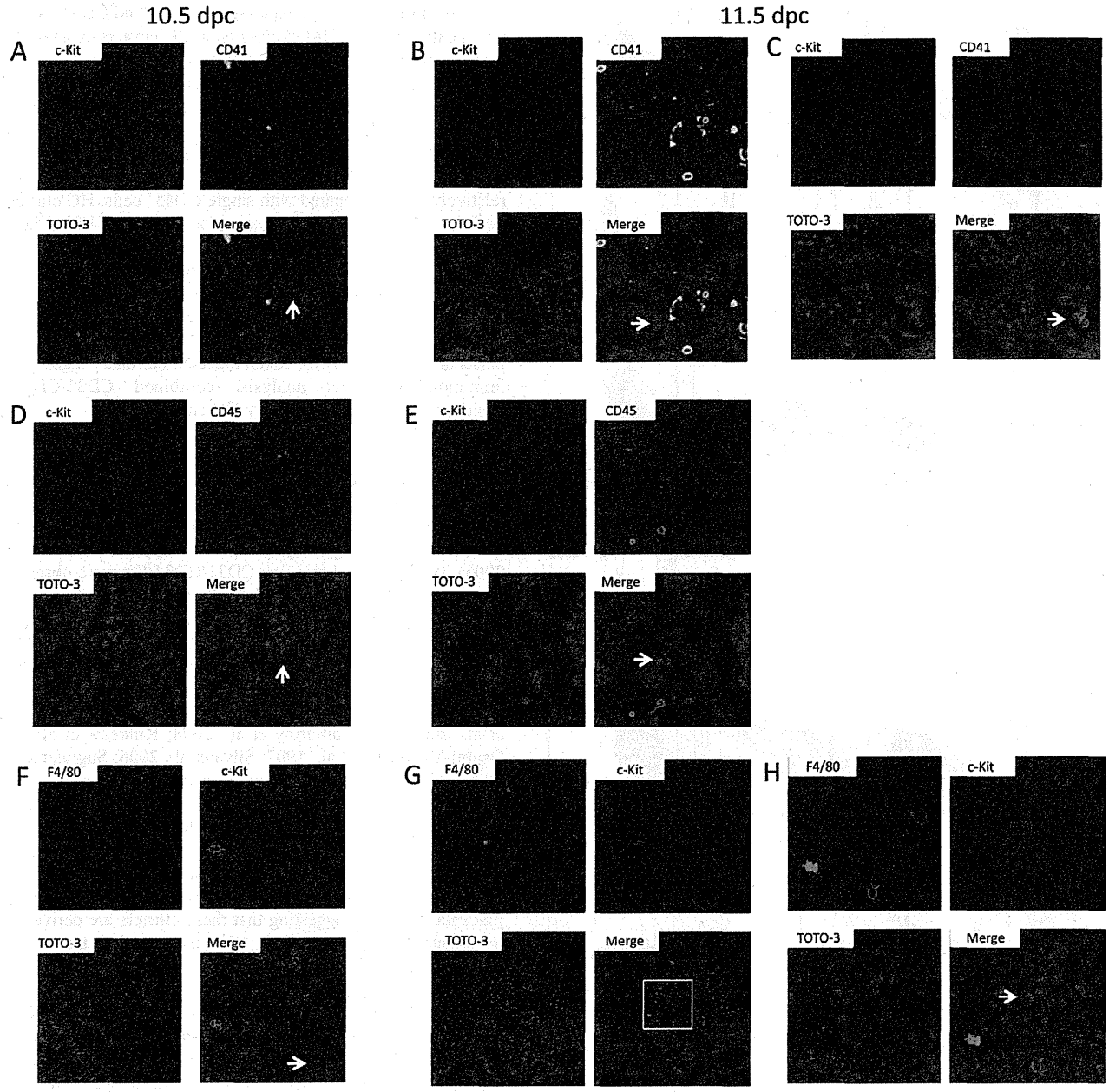

Fig. 3. Confocal images of CD41, CD45 and F4/80 placental expression. Placenta sections were made from ICR mouse embryos both at 10.5 and 11.5 dpc, stained with antibodies and observed under confocal microscopy. (A,D) Images of 10.5 dpc placenta. (B,C,E-H) Images of 11.5 dpc placenta. (**A-C**) Sections were stained with anti-Kit antibody (red), anti-CD41 antibody (green) and TOTO-3 (blue). (A) HC cluster at 10.5 dpc expressed Kit, but not CD41. Arrow indicates HC cluster. (B) HC cluster at 11.5 dpc expressed Kit but not CD41. Some single cells strongly expressed CD41. Arrow indicates HC cluster. (C) HC cluster at 11.5 dpc expressing both Kit and CD41. The intensity of CD41 expression was relatively weak. Arrow indicates HC cluster. (**D**,**E**) Sections were stained with anti-Kit antibody (red), anti-CD45 antibody (green) and TOTO-3 (blue). (D) HC cluster at 10.5 dpc expressing Kit, but not CD45. Arrow indicates HC cluster. (E) HC cluster at 11.5 dpc expressed both Kit and CD45. The intensity of CD45 expression was relatively weak. Arrow indicates HC cluster. (**F-H**) Sections were stained with anti-F4/80 antibody (red), anti-Kit antibody (green) and TOTO-3 (blue). (F) HC cluster at 10.5 dpc expressing Kit, but not F4/80. Arrow indicates a $Kit^{-}/F4/80^{+}$ cell. (G) Blood vessel at 11.5 dpc. Some single cells expressed F4/80. (H) High magnification view of boxed area in G. Arrow indicates $c\text{-}Kit^{+}/F4/80^{+/+}$ cell circulating inside of blood vessel. For all images, original magnification is ×40.

Regulation of HC clusters by niche cells

To investigate extrinsic factors that regulate HC cluster proliferation, we used an LCM system to collect niche cells surrounding HC clusters expressing Kit at 11.5 dpc. This technique enables us to isolate precisely specific cell compartments in tissue sections (Gomez and Harrison, 2009). The experimental strategy is shown in Fig. S4 in the supplementary material. We obtained niche cells comprising both endothelial and

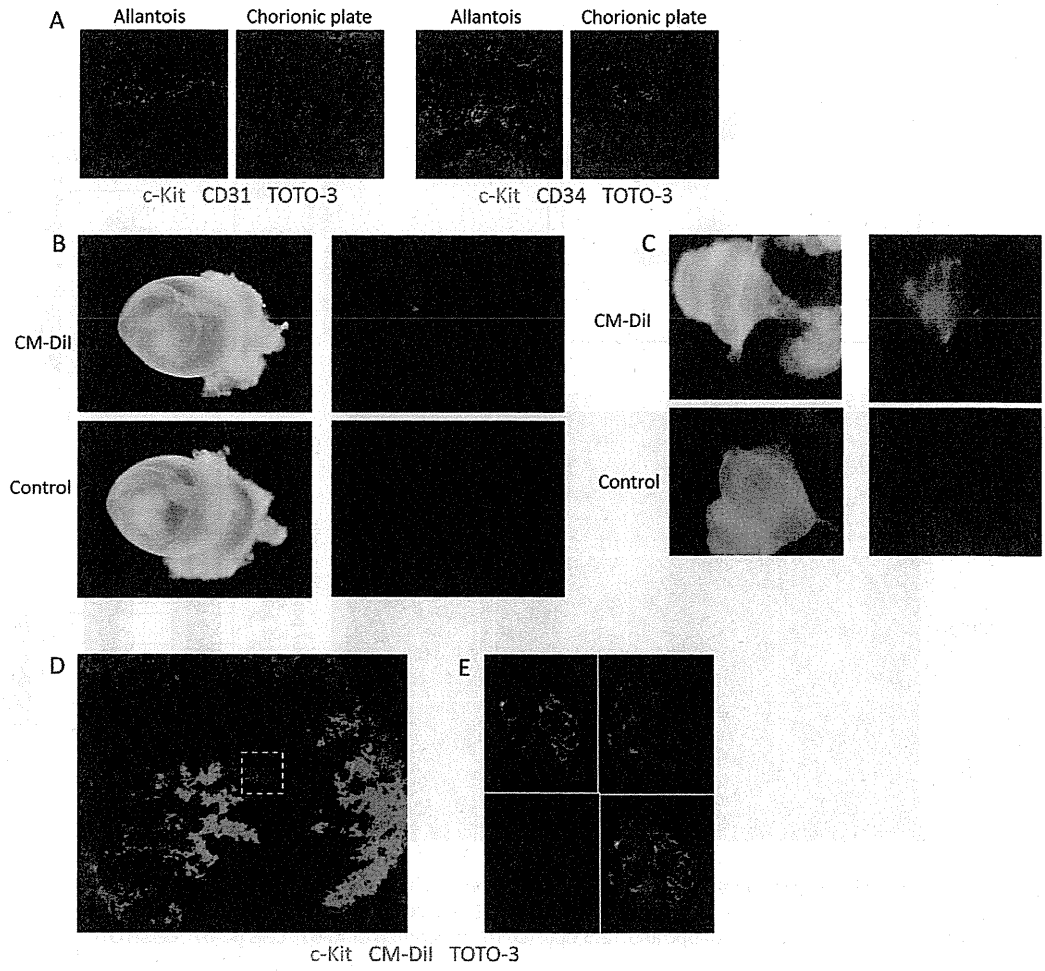

Fig. 4. Origin of placental HC clusters. (**A**) Sections of placenta were made from ICR mouse embryos at 9.5 dpc. Confocal image of HC clusters expressing CD31/CD34/Kit in the allantois and chorionic plate at 9.5 dpc. (**B**) CM-DiI was injected into the basal part of allantois of ICR mouse embryos at 8.25 dpc before chorio-allantoic fusion. Injected embryos are shown under a standard stereomicroscope (left) and under a fluorescence stereomicroscope (right). (**C**) CM-DiI tagged embryos subjected to whole embryo culture for 42 hours are shown under a stereomicroscope (left) and a fluorescence stereomicroscope (right). Upper panels show CM-DiI tagged embryo; lower panels show a non-tagged control. (**D**) The placenta of a CM-DiI tagged embryo after 42 hours culture was immunostained with anti-Kit antibody. Expression of Kit (green), CM-DiI (red) and TOTO-3 (blue) was observed by confocal microscopy. (**E**) High magnification view of an HC cluster (boxed area in D).

mesenchymal cells. To collect total RNAs by LCM in numbers sufficient to perform further analysis meant that we had to shorten the immunostaining period. We also could not use confocal microscopy to visualize HC clusters due to hardware limitations. We found that among Kit, CD31, CD34 and CD41 antibodies, the Kit antibody was most sensitive and specific to stain sections quickly and identify small HC clusters. Expression of hematopoietic cytokine genes such as SCF, *Tpo*, *Flt3l*, *Il3*, *Il6*, *Il11*, GM-CSF (*Csf2* – Mouse Genome Informatics), G-CSF (*Csf3* – Mouse Genome Informatics), *Epo* and *Osm* (see Fig. 6A legend for abbreviations) was evaluated by real-time PCR in isolated niche cells (Fig. 6A). SCF, *Tpo*, *Flt3l*, *Il6*, GM-CSF and *Osm* expression was detected in placental tissue containing various cell types. When we compared isolated niche cells with placental cells, SCF expression was four times higher in niche compared with placental cells, suggesting that SCF is a potential extrinsic factor regulating HC cluster proliferation. To further characterize placental niche cells, we used flow cytometry to sort endothelial cells and mesenchymal cells from both placenta at 11.5 dpc and the AGM region at 10.5 dpc, as HC clusters are prominent at 10.5 dpc and disappear by 11.5 dpc in the AGM region, whereas HC clusters are apparent at 11.5 dpc in the placenta (Godin and Cumano, 2002). The endothelial cell population was defined as $CD31^+/CD34^+/Kit^-/Ter119^-/CD45^-$ and the mesenchymal as $CD31^-/CD34^-/Kit^-/Ter119^-/CD45^-$ (Fig. 6B). When we analyzed expression of SCF, *Tpo*, *Flt3l* and *Il6* by real-time PCR, SCF expression was detected primarily in both endothelial and mesenchymal cells of the placenta and AGM region (Fig. 6C). SCF expression levels in endothelial cells were 2.5-fold and 8-fold higher than in mesenchymal cells in the placenta and AGM region, respectively. To confirm SCF protein expression, we undertook ELISA analysis and detected SCF only in placental

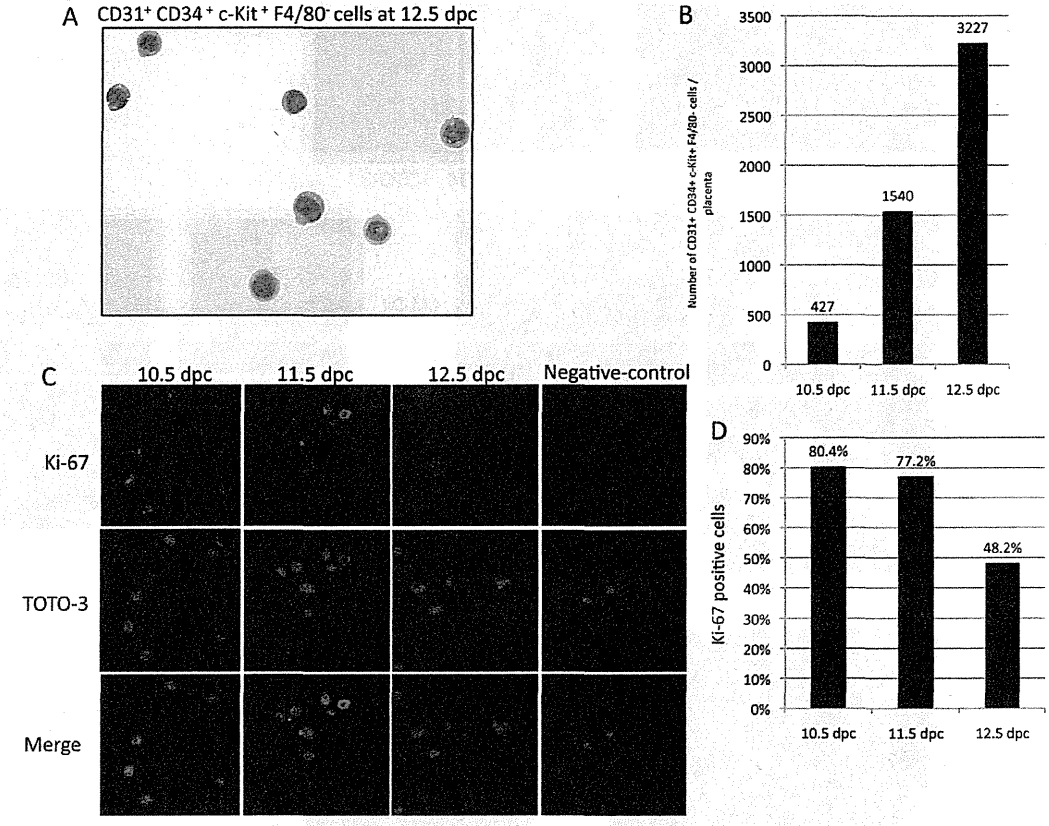

Fig. 5. Analysis of proliferation in placental HC clusters. (**A**) Morphology of CD31$^+$/CD34$^+$/Kit$^+$/F4/80$^-$ cells at 12.5 dpc. (**B**) The number of CD31$^+$/CD34$^+$/Kit$^+$/F4/80$^-$ cells per placenta at 10.5 dpc, 11.5 dpc and 12.5 dpc. (**C**) Confocal image demonstrating Ki-67 expression in CD31$^+$/CD34$^+$/Kit$^+$/F4/80$^-$ cells at 10.5 dpc, 11.5 dpc and 12.5 dpc. (**D**) The proportion of Ki-67$^+$ cells (Ki-67$^+$ cells/TOTO-3$^+$ cells) at 10.5 dpc, 11.5 dpc and 12.5 dpc.

endothelial cells (0.49 ng/10^3 cells) and in the AGM region (0.95 ng/10^3 cells) (Fig. 6D). To determine which endothelial cells expressed SCF, we also evaluated co-expression of SCF with CD31 or CD34 at 11.5 dpc. Expression of SCF protein was observed associated with capillary vessels expressing CD31 or CD34, but not in all endothelial cells (Fig. 6E,F). In particular, endothelial cells attached to HC clusters expressed SCF, suggesting that endothelial cells surrounding HC clusters function as niche cells through SCF expression. To investigate whether SCF/Kit signaling regulates HC clusters in the placenta, we administered an anti-Kit neutralizing antibody (ACK2) by intracardiac injection to embryos at 10.25 dpc (Czechowicz et al., 2007; Ogawa et al., 1993). Injected embryos were then cultured in a WEC system for 6 hours (Sugiyama et al., 2003; Kulkeaw et al., 2009). Following culture, injected embryos were harvested and their placentas dissociated for flow cytometric analysis. Cells expressing CD31+/CD34+/Kit+ (equivalent to HC clusters) were flow sorted and expression of hematopoietic transcription factors SCL (*Tal1* – Mouse Genome Informatics), *Runx1*, *Myb* and *Gata2* was examined by real-time PCR (Fig. 7). When compared with a control sample from embryos injected with isotype control IgG, expression of *Runx1*, *Myb* and *Gata2* was significantly downregulated, whereas that of SCL was unchanged. These data suggest that SCF/Kit signaling regulates HC clusters through *Runx1*, *Myb* and *Gata2*.

DISCUSSION

Localization of HC clusters in placenta

To examine mechanisms governing niche cell regulation of HSCs in the mouse placenta, it was necessary to gain insights into their cellular interactions through observation of their morphology and evaluating cells based on marker expression. Previous studies have characterized placental HSCs primarily by flow cytometry, cell culture and transplantation (Alvarez-Silva et al., 2003; Gekas et al., 2005), while immunohistochemical analysis of HC clusters has not been extensively undertaken. We successfully identified Kit$^+$/CD31$^+$/CD34$^+$ HC clusters in the mouse placenta and AGM region. Clusters in the placenta were attached to endothelial cells, as has been observed in the AGM region, a site of HSC generation, suggesting that the placenta might be a site for HSC generation. We determined whether HSC surface markers, such as CD41 (Corbel and Salaun, 2002; Corbel et al., 2005; Ferkowicz et al., 2003; Matsubara et al., 2005; Mikkola et al., 2003a; Mitjavila-Garcia et al., 2002), CD45 (Matsubara et al., 2005; North et al., 2002), EPCR (CD201) (Balazs et al., 2006) and Sca-1 (de Bruijn et al., 2002) were expressed in placental HC clusters using flow cytometry. Although 59.8% of CD31$^+$/CD34$^+$/Kit$^+$/F4/80$^-$ cells expressed CD41 when analyzed by flow cytometry (Fig. 2), no strong CD41 signal on HC clusters was detected by immunohistochemstry at 10.5 dpc (Fig. 3). Another group has used an enzyme/antibody technique to stain HC clusters, whereas we employed fluorescent

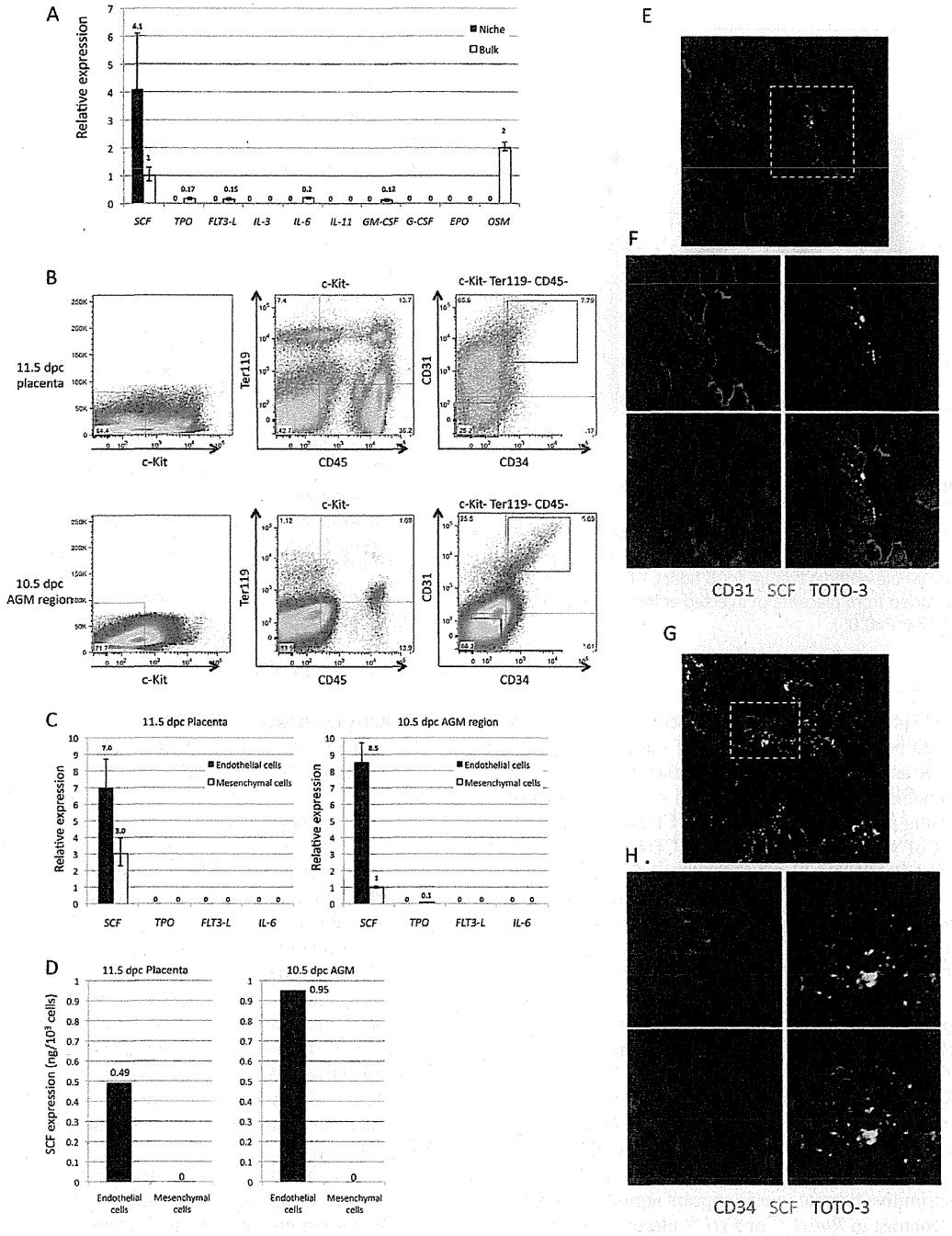

Fig. 6. Cytokine expression in niche cells. (**A**) Relative expression of cytokine genes in niche cells isolated by LCM indicated as 'Niche' (black bar), compared with placental tissue indicated as 'Bulk' (white bar). SCF, stem cell factor; TPO, thrombopoietin; FLT3-L, Flt3-ligand; IL3, interleukin 3) IL6, interleukin 6; IL11, interleukin 11; GM-CSF, granulocyte-macrophage colony stimulating factor; G-CSF, granulocyte colony stimulating factor; EPO, erythropoietin; OSM, oncostatin M. (**B**) Sorting by flow cytometry of endothelial ($CD31^{+}/CD34^{+}/Kit^{-}/Ter119^{-}/CD45^{-}$) and mesenchymal cells ($CD31^{-}/CD34^{-}/Kit^{-}/Ter119^{-}/CD45^{-}$) from the placenta at 11.5 dpc and the AGM region at 10.5 dpc. (**C**) Relative expression of SCF, TPO, *Flt3l* and *Il6* genes in placental endothelial and mesenchymal cells at 11.5 dpc placenta and the AGM region at 10.5 dpc. (**D**) Expression of SCF protein (ng/10^3 cells) measured by ELISA in placental endothelial and mesenchymal cells at 11.5 dpc and the AGM region at 10.5 dpc. (**E-H**) Placenta sections were made from ICR mouse embryos at 11.5 dpc, stained with antibodies and observed under confocal microscopy. The antibody combination is as follows. (E,F) CD31 (red), SCF (green) and TOTO-3 (blue). (G,H) CD34 (red), SCF (green) and TOTO-3 (blue). Confocal images demonstrate placental localization of SCF at 11.5 dpc. (F,H) Higher magnification view of boxed areas in E and G, respectively. (E) SCF is expressed in endothelial cells surrounding HC clusters that express CD31. (G) SCF is expressed in HC clusters in addition to endothelial cells that express CD34.

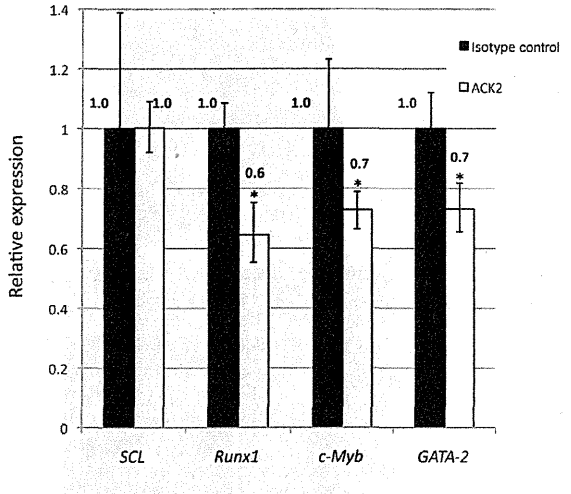

Fig. 7. Altered *Runx1, Myb* and *Gata2* expression in CD31$^+$/CD34$^+$/Kit$^+$ cells following inhibition of placental SCF/Kit signaling. Intra-cardiac injection of ACK2, a neutralizing antibody, was used to block Kit receptor function in 10.25 dpc mouse embryos followed by whole-embryo culture for 6 hours. CD31$^+$/CD34$^+$/Kit$^+$ cells were flow sorted from placenta of injected embryos and analyzed by real-time PCR (*P<0.05).

antibodies (Rhodes et al., 2008). The discrepancy and difference in results might be due to the difference of staining method or to the nature of the antibody, i.e. either appropriate for flow cytometry or for immunohistochemistry. We found we could identify HC clusters using a combination of CD31, CD34 and Kit antibodies, regardless of whether they expressed CD41 or CD45. We also investigated HC clusters in the placenta of *Runx1*$^{-/-}$, *Evi1*$^{-/-}$ or *Myb*$^{-/-}$ mouse embryos. Runx1 is essential for definitive hematopoiesis, and its expression marks the site of de novo generation of hematopoietic progenitors (North et al., 1999; Okuda et al., 1996; Wang et al., 1996). We observed an absence of HC clusters in *Runx1*$^{-/-}$ placentas. Evi1 is important for HSC generation and expansion, and HSC development in the para-aortic-splanchnopleural mesoderm (P-Sp) region is severely impaired in *Evi1*$^{-/-}$ embryos (Goyama et al., 2008; Yuasa et al., 2005). Similar to our observations of *Runx1*$^{-/-}$ embryos, we detected no HC clusters in the *Evi1*$^{-/-}$ placenta. Myb is essential for HSC maturation and proliferation, and *Myb*$^{-/-}$ embryos die at 15.5 dpc from impaired definitive hematopoiesis in the fetal liver, although primitive hematopoiesis appears normal (Mucenski et al., 1991). In contrast to *Runx1*$^{-/-}$ or *Evi1*$^{-/-}$ placenta, we observed HC clusters in the *Myb*$^{-/-}$ placenta, and these clusters were larger than those seen in wild-type animals. Although *Myb*$^{-/-}$ embryos can form endothelial sheet, they fail to generate hematopoietic cells in vitro (Mukoyama et al., 1999). Taken together with our result, they might lack the potential of differentiation from HC clusters to relatively mature hematopoietic cells. Overall, abnormal HC cluster formation seen in knockout mouse embryos indicates that the placenta plays an important role in that process.

In the placental vasculature, the presence of HC clusters composed of up to ten cells has been reported previously (Ottersbach and Dzierzak, 2005; Rhodes et al., 2008). However, we identified larger HC clusters, comprising more than 30 cells, as well as surrounding cells by using thick placental cryosections (20 μm) and confocal microscopy. This methodology might also be useful to investigate interactions between HSCs and surrounding cells in other hematopoietic organs.

Flow cytometric analysis of placental cells

Although we visualized HC clusters by immunohistochemistry, HC clusters expressing CD31, CD34 and Kit may contain hematopoietic progenitors. CD34$^+$/Kit$^+$ cells in the placenta at E12.5 reportedly contain HSCs and hematopoietic progenitors (Gekas et al., 2005). This finding suggests that a combination of CD31, CD34 and Kit antibodies is sufficient to identify HC clusters by morphology, but not specific for HSCs. Therefore, our clusters probably contain both HSCs and progenitors. Although flow cytometry could be employed to purify these two cell populations, those preparations could be contaminated by circulating hematopoietic cells or other cell types. It has been reported that F4/80$^+$ macrophages populate the placental mesenchyme (Rhodes et al., 2010). In agreement, we observed some single F4/80$^+$ cells in the mesenchyme, in addition to c-Kit$^+$/F4/80$^{+/+}$ cells in circulation in the placenta (Fig. 3). Therefore, after removing F4/80$^+$ cells from the CD31$^+$/CD34$^+$/Kit$^+$ population, we considered that the remaining clusters contained primarily HSCs and hematopoietic progenitors. Our data suggest that a combination of CD31, CD34 and Kit antibodies can be employed to identify HC clusters, regardless of contamination by mature macrophages. By combining CD41 with CD31, CD34 and Kit to sort HC clusters by flow cytometry, we may be able to purify HSCs from this population.

Origin of placental HSCs

Although the YS, AGM region and FL are well recognized organs for hematopoiesis, the small number of HSCs generated in the YS and AGM region cannot completely account for the number of HSCs in FL prior to HSC expansion. In addition, there is a 2-day time lag between HSC generation in the AGM and initiation of HSC expansion in FL. These observations suggest the presence of another hematopoietic site for HSC generation to fill a time gap between AGM region and FL (Kumaravelu et al., 2002). In avian embryos, quail-chick grafting experiments have demonstrated that the allantois (which is equivalent to mammalian placenta) generates definitive hematopoietic cells de novo (Caprioli et al., 1998; Caprioli et al., 2001). It has also been reported that mouse placenta contains HSCs and hematopoietic progenitors (Gekas et al., 2005; Ottersbach and Dzierzak, 2005). The hematopoietic potential of the allantois and chorion isolated prior to establishment of circulation and their fusion has been studied in the mouse placenta (Corbel et al., 2007; Zeigler et al., 2006). These studies showed that both the allantois and chorion exhibit myelo-erythroid potential, implying that definitive hematopoiesis occurs in the placenta. The presence of myelo-erythroid and B- and T-cell progenitors in the placenta of *Ncx1*$^{-/-}$ mouse embryos, which lack a heartbeat and therefore input from circulating cells to the placenta, supports the notion that HSCs are autonomously generated (Rhodes et al., 2008). However, in vivo experiments to examine the origin of HSCs in mouse placenta has not been performed owing to the difficulty in manipulating embryos within a thick uterine membrane. To overcome this problem, we used a WEC system, enabling us to follow events outside the uterus in vivo (Kulkeaw et al., 2009). When four embryos injected with CM-DiI at 8.25 dpc were cultured in WEC for 42 hours, all developed an umbilical cord and placenta. Here, we determined the origin of HC clusters in the placenta by tagging the allantois at 8.25 dpc with CM-DiI and culturing injected mouse embryos. All Kit$^+$ cell aggregates were CM-DiI$^+$, and no Kit$^+$

aggregate was DiI-negative, although some single CM-DiI$^-$/Kit$^+$ cells were observed (data not shown). It is possible that not all allantoic cells were CM-DiI-tagged and that non-tagged cells gave rise to single Kit$^+$ cells, given the technical difficulty of tagging all cells. We injected CM-DiI into the basal part of allantois, implying that HC clusters are originated from this part. It is also possible that chorionic cells per se may give rise to Kit$^+$ cells: chorion reportedly has a potential to generate myeloid and definitive erythroid cells (Corbel et al., 2007; Zeigler et al., 2006). Thus, although some HC clusters may have been derived from chorion, it is more likely that the mouse placenta does autonomously generate HSCs and that the allantois is at least a major source of placental HSCs. As shown in Fig. 4A, HC clusters first form cell aggregates. Although several reports suggest that HC clusters in the AGM region are derived from endothelial cells expressing VE-cadherin (Dzierzak and Speck, 2008), the HC clusters in the placenta probably did not originate from endothelial cells. Interestingly, Fraser et al. demonstrated that VE-cadherin is also expressed in HC clusters in the AGM region, indicating that VE-cadherin is not a specific marker of endothelial cells (Fraser et al., 2003). It may be further necessary to evaluate the origin of HC clusters both in the AGM region and the placenta in the future.

Niche regulation of placental HSCs

HSCs are regulated by niche cells surrounding HSCs. However, it remains unclear how embryonic HSCs are regulated by niche cells. In the bone marrow, expression of niche cell markers such as N-cadherin and CXCL12 enables their isolation by flow cytometry and has contributed greatly to an understanding of niche regulation (Arai and Suda, 2007; Sugiyama et al., 2006). Conversely, investigation of the placental niche has been impeded by a lack of markers for placental niche cells. To address this issue, we isolated niche cells surrounding HC clusters in placenta by LCM. Using this system, we obtained niche cells despite the lack of markers. HC clusters were found inside blood vessels, suggesting that niche cells are mostly composed of endothelial cells. In addition, we sorted out both endothelial and mesenchymal cells, and performed real-time PCR with SCF gene (Fig. 6). Our gene expression analysis revealed that SCF is predominantly expressed in niche cells, and protein expression analysis suggested that SCF is predominantly expressed in niche endothelial cells. In agreement, we found that SCF is predominantly expressed in endothelial cells, in particular cells surrounding HC clusters by immunostaining. Interestingly, SCF was expressed in clusters as well as in endothelial cells, implying an autocrine mechanism. It would be of interest to investigate whether SCF plays a role in specification as well as niche development. To understand the role of the SCF/Kit signal in regulating placental HSCs, we performed a loss-of-function experiment in vivo to inhibit SCF/Kit signaling in the mouse placenta using a WEC system with 10.25 dpc embryos – a stage suitable for manipulation. SCL is not required for HSC development once commitment to hematopoietic lineages has occurred (D'Souza et al., 2005; Mikkola et al., 2003b; Robb et al., 1995; Shivdasani et al., 1995). However, Gata2 is crucial for definitive hematopoiesis and functions in the generation and expansion of HSCs in the AGM region (Ling et al., 2004; Lugus et al., 2007; Tsai et al., 1994). Our study confirmed that expression of *Runx1*, *Myb* and *Gata2* was significantly downregulated compared with control samples in Kit loss-of-function analyses but *SCL* expression was not altered. Kit receptor activation plays a major role in regulating survival, proliferation and self-renewal of HSC phenotypes (Kent et al., 2008), but how SCF/Kit signal regulates *Runx1*, *Myb* and *Gata2* remains unclear. In addition to SCF/Kit signaling, other signals may regulate HC clusters. SCF secreted by niche cells may modulate proliferation of CD31$^+$/CD34$^+$/Kit$^+$ cells between 10.5 and 12.5 dpc, as shown in Fig. 5, although this proliferation might be due to an accumulation of the hematopoietic cells in the placental vasculature as this organ increases in size. Decrease of Ki-67 positive cells might be due to the downregulation of SCF by niche cells.

IL3 reportedly increases the number of HSCs in the AGM region (Robin et al., 2006). However, these authors demonstrated that IL3 has no effect on HSC activity in the placenta at 10.5 dpc, an observation compatible with our data showing that IL3 is not expressed in placental niche cells (Fig. 6A). Hedgehog, BMP4, bFGF and VEGF signals from the surrounding micro-environment are required for mesodermal cells to commit to hematopoietic cells (Dzierzak and Speck, 2008). In the AGM region, location plays a role in regulating HSC generation: ventral tissues induce AGM HSCs, whereas dorsal tissues suppress them (Peeters et al., 2009). Hedgehog protein(s) have been identified as positive effectors that increase the number of AGM HSCs (Peeters et al., 2009). Moreover, there is greater expansion of placental HSCs from 11.5 dpc to 12.5 dpc than of hematopoietic progenitors at this site, suggesting that other signals in the placental niche probably inhibit HSC differentiation (Gekas et al., 2005).

This is the first report to identify and examine the function of cytokine signals regulating HSCs in the mouse placenta. Our study is also evidence that LCM is a useful tool with which to study molecular mechanisms in specific cell aggregates. Recently, it was demonstrated that human placenta contains HSCs and that stromal cells (derived from human placenta) could support hematopoiesis (Robin et al., 2009). Clarifying how the niche regulates HSCs in the placenta could lead to an understanding of how to manipulate HSC generation from ES/iPS cells and, thus, be applicable to future clinical applications.

Acknowledgements

This research was partially supported by a Grant-in-Aid for Exploratory Research; by the Project for Realization of Regenerative Medicine; by Special Coordination Funds for Promoting Science and Technology of the Ministry of Education, Science, Sports and Culture; and by a Bilateral Program of the Japan Society for the Promotion of Science. We thank the Research Support Center, Graduate School of Medical Sciences, Kyushu University for technical support; Drs M. Ogawa, C. Meno and S. Oki for helpful discussion; Dr R. Jones for critical reading of our manuscript; and Drs K. Kulkeaw and T. Inoue for technical support in our laboratory.

Competing interests statement

The authors declare no competing financial interests.

Supplementary material

Supplementary material for this article is available at http://dev.biologists.org/lookup/suppl/doi:10.1242/dev.051359/-/DC1

References

Alvarez-Silva, M., Belo-Diabangouaya, P., Salaun, J. and Dieterlen-Lievre, F. (2003). Mouse placenta is a major hematopoietic organ. *Development* **130**, 5437-5444.

Arai, F. and Suda, T. (2007). Maintenance of quiescent hematopoietic stem cells in the osteoblastic niche. *Ann. NY Acad. Sci.* **1106**, 41-53.

Balazs, A. B., Fabian, A. J., Esmon, C. T. and Mulligan, R. C. (2006). Endothelial protein C receptor (CD201) explicitly identifies hematopoietic stem cells in murine bone marrow. *Blood* **107**, 2317-2321.

Baumann, C. I., Bailey, A. S., Li, W., Ferkowicz, M. J., Yoder, M. C. and Fleming, W. H. (2004). PECAM-1 is expressed on hematopoietic stem cells throughout ontogeny and identifies a population of erythroid progenitors. *Blood* **104**, 1010-1016.

Caprioli, A., Jaffredo, T., Gautier, R., Dubourg, C. and Dieterlen-Lievre, F. (1998). Blood-borne seeding by hematopoietic and endothelial precursors from the allantois. *Proc. Natl. Acad. Sci. USA* **95**, 1641-1646.

Caprioli, A., Minko, K., Drevon, C., Eichmann, A., Dieterlen-Lievre, F. and Jaffredo, T. (2001). Hemangioblast commitment in the avian allantois: cellular and molecular aspects. *Dev. Biol.* **238**, 64-78.
Corbel, C. and Salaun, J. (2002). Alphallb integrin expression during development of the murine hemopoietic system. *Dev. Biol.* **243**, 301-311.
Corbel, C., Vaigot, P. and Salaun, J. (2005). (alpha)IIb Integrin, a novel marker for hemopoietic progenitor cells. *Int. J. Dev. Biol.* **49**, 279-284.
Corbel, C., Salaun, J., Belo-Diabangouaya, P. and Dieterlen-Lievre, F. (2007). Hematopoietic potential of the pre-fusion allantois. *Dev. Biol.* **301**, 478-488.
Cumano, A., Dieterlen-Lievre, F. and Godin, I. (1996). Lymphoid potential, probed before circulation in mouse, is restricted to caudal intraembryonic splanchnopleura. *Cell* **86**, 907-916.
Cudennec, C. A., Thiery, J. P. and Le Douarin, N. (1981). In vitro induction of adult erythropoiesis in early mouse yolk sac. *Proc. Natl. Acad. Sci. USA* **78**, 2412-2416.
Czechowicz, A., Kraft, D., Weissman, I. L. and Bhattacharya, D. (2007). Efficient transplantation via antibody-based clearance of hematopoietic stem cell niches. *Science* **318**, 1296-1299.
D'Souza, S. L., Elefanty, A. G. and Keller, G. (2005). SCL/Tal-1 is essential for hematopoietic commitment of the hemangioblast but not for its development. *Blood* **105**, 3862-3870.
Dancis, J., Jansen, V., Gorstein, F. and Douglas, G. W. (1968). Hematopoietic cells in mouse placenta. *Am. J. Obstet. Gynecol.* **100**, 1110-1121.
Dancis, J., Jansen, V., Brown, G. F., Gorstein, F. and Balis, M. E. (1977). Treatment of hypoplastic anemia in mice with placental transplants. *Blood* **50**, 663-670.
de Bruijn, M. F., Ma, X., Robin, C., Ottersbach, K., Sanchez, M. J. and Dzierzak, E. (2002). Hematopoietic stem cells localize to the endothelial cell layer in the midgestation mouse aorta. *Immunity* **16**, 673-683.
Downs, K. and Harmann, C. (1997). Developmental potency of the murine allantois. *Development* **124**, 2769-2780.
Dzierzak, E. and Speck, N. A. (2008). Of lineage and legacy: the development of mammalian hematopoietic stem cells. *Nat. Immunol.* **9**, 129-136.
Ema, H. and Nakauchi, H. (2000). Expansion of hematopoietic stem cells in the developing liver of a mouse embryo. *Blood* **95**, 2284-2288.
Ferkowicz, M. J. and Yoder, M. C. (2005). Blood island formation: longstanding observations and modern interpretations. *Exp. Hematol.* **33**, 1041-1047.
Ferkowicz, M. J., Starr, M., Xie, X., Li, W., Johnson, S. A., Shelley, W. C., Morrison, P. R. and Yoder, M. C. (2003). CD41 expression defines the onset of primitive and definitive hematopoiesis in the murine embryo. *Development* **130**, 4393-4403.
Fraser, S. T., Ogawa, M., Yokomizo, T., Ito, Y., Nishikawa, S. and Nishikawa, S. (2003). Putative intermediate precursor between hematogenic endothelial cells and blood cells in the developing embryo. *Dev. Growth Differ.* **45**, 63-75.
Gekas, C., Dieterlen-Lievre, F., Orkin, S. H. and Mikkola, H. K. (2005). The placenta is a niche for hematopoietic stem cells. *Dev. Cell* **8**, 365-375.
Godin, I. and Cumano, A. (2002). The hare and the tortoise: an embryonic haematopoietic race. *Nat. Rev. Immunol.* **2**, 593-604.
Gomez, S. K. and Harrison, M. J. (2009). Laser microdissection and its application to analyze gene expression in arbuscular mycorrhizal symbiosis. *Pest Manage. Sci.* **65**, 504-511.
Goyama, S., Yamamoto, G., Shimabe, M., Sato, T., Ichikawa, M., Ogawa, S., Chiba, S. and Kurokawa, M. (2008). Evi-1 is a critical regulator for hematopoietic stem cells and transformed leukemic cells. *Cell Stem Cell* **3**, 207-220.
Houssaint, E. (1981). Differentiation of the mouse hepatic primordium. II. Extrinsic origin of the haemopoietic cell line. *Cell Differ.* **10**, 243-252.
Johnson, G. R. and Moore, M. A. (1975). Role of stem cell migration in initiation of mouse foetal liver haemopoiesis. *Nature* **258**, 726-728.
Kent, D., Copley, M., Benz, C., Dykstra, B., Bowie, M. and Eaves, C. (2008). Regulation of hematopoietic stem cells by the steel factor/KIT signaling pathway. *Clin. Cancer Res.* **14**, 1926-1930.
Khakoo, A. Y., Pati, S., Anderson, S. A., Reid, W., Elshal, M. F., Rovira, I. I., Nguyen, A. T., Malide, D., Combs, C. A., Hall, G. et al. (2006). Human mesenchymal stem cells exert potent antitumorigenic effects in a model of Kaposi's sarcoma. *J. Exp. Med.* **203**, 1235-1247.
Krishnamurthy, K., Wang, G., Rokhfeld, D. and Bieberich, E. (2008). Deoxycholate promotes survival of breast cancer cells by reducing the level of pro-apoptotic ceramide. *Breast Cancer Res.* **10**, R106.
Kulkeaw, K., Mizuochi, C., Horio, Y., Osumi, N., Tsuji, K. and Sugiyama, D. (2009). Application of whole mouse embryo culture system on stem cell research. *Stem Cell Rev.* **5**, 175-180.
Kumaravelu, P., Hook, L., Morrison, A. M., Ure, J., Zhao, S., Zuyev, S., Ansell, J. and Medvinsky, A. (2002). Quantitative developmental anatomy of definitive haematopoietic stem cells/long-term repopulating units (HSC/RUs): role of the aorta-gonad-mesonephros (AGM) region and the yolk sac in colonisation of the mouse embryonic liver. *Development* **129**, 4891-4899.
Li, W., Johnson, S. A., Shelley, W. C., Ferkowicz, M., Morrison, P., Li, Y. and Yoder, M. C. (2003). Primary endothelial cells isolated from the yolk sac and para-aortic splanchnopleura support the expansion of adult marrow stem cells in vitro. *Blood* **102**, 4345-4353.
Ling, K. W., Ottersbach, K., van Hamburg, J. P., Oziemlak, A., Tsai, F. Y., Orkin, S. H., Ploemacher, R., Hendriks, R. W. and Dzierzak, E. (2004). GATA-2 plays two functionally distinct roles during the ontogeny of hematopoietic stem cells. *J. Exp. Med.* **200**, 871-882.
Lugus, J. J., Chung, Y. S., Mills, J. C., Kim, S. I., Grass, J., Kyba, M., Doherty, J. M., Bresnick, E. H. and Choi, K. (2007). GATA2 functions at multiple steps in hemangioblast development and differentiation. *Development* **134**, 393-405.
Matsubara, A., Iwama, A., Yamazaki, S., Furuta, C., Hirasawa, R., Morita, Y., Osawa, M., Motohashi, T., Eto, K., Ema, H. et al. (2005). Endomucin, a CD34-like sialomucin, marks hematopoietic stem cells throughout development. *J. Exp. Med.* **202**, 1483-1492.
Matsuoka, S., Tsuji, K., Hisakawa, H., Xu, M., Ebihara, Y., Ishii, T., Sugiyama, D., Manabe, A., Tanaka, R., Ikeda, Y. et al. (2001). Generation of definitive hematopoietic stem cells from murine early yolk sac and paraaortic splanchnopleures by aorta-gonad-mesonephros region-derived stromal cells. *Blood* **98**, 6-12.
McGrath, K. E. and Palis, J. (2005). Hematopoiesis in the yolk sac: more than meets the eye. *Exp. Hematol.* **33**, 1021-1028.
Medvinsky, A. and Dzierzak, E. (1996). Definitive hematopoiesis is autonomously initiated by the AGM region. *Cell* **86**, 897-906.
Melchers, F. (1979). Murine embryonic B lymphocyte development in the placenta. *Nature* **277**, 219-221.
Mikkola, H. K., Fujiwara, Y., Schlaeger, T. M., Traver, D. and Orkin, S. H. (2003a). Expression of CD41 marks the initiation of definitive hematopoiesis in the mouse embryo. *Blood* **101**, 508-516.
Mikkola, H. K., Klintman, J., Yang, H., Hock, H., Schlaeger, T. M., Fujiwara, Y. and Orkin, S. H. (2003b). Haematopoietic stem cells retain long-term repopulating activity and multipotency in the absence of stem-cell leukaemia SCL/tal-1 gene. *Nature* **421**, 547-551.
Mitjavila-Garcia, M. T., Cailleret, M., Godin, I., Nogueira, M. M., Cohen-Solal, K., Schiavon, V., Lecluse, Y., Le Pesteur, F., Lagrue, A. H. and Vainchenker, W. (2002). Expression of CD41 on hematopoietic progenitors derived from embryonic hematopoietic cells. *Development* **129**, 2003-2013.
Mucenski, M. L., McLain, K., Kier, A. B., Swerdlow, S. H., Schreiner, C. M., Miller, T. A., Pietryga, D. W., Scott, W. J., Jr and Potter, S. S. (1991). A functional c-myb gene is required for normal murine fetal hepatic hematopoiesis. *Cell* **65**, 677-689.
Mukouyama, Y., Chiba, N., Mucenski, M. L., Satake, M., Miyajima, A., Hara, T. and Watanabe, T. (1999). Hematopoietic cells in cultures of the murine embryonic aorta-gonad-mesonephros region are induced by c-Myb. *Curr. Biol.* **9**, 833-836.
North, T., Gu, T. L., Stacy, T., Wang, Q., Howard, L., Binder, M., Marin-Padilla, M. and Speck, N. A. (1999). Cbfa2 is required for the formation of intra-aortic hematopoietic clusters. *Development* **126**, 2563-2575.
North, T. E., de Bruijn, M. F., Stacy, T., Talebian, L., Lind, E., Robin, C., Binder, M., Dzierzak, E. and Speck, N. A. (2002). Runx1 expression marks long-term repopulating hematopoietic stem cells in the midgestation mouse embryo. *Immunity* **16**, 661-672.
Ogawa, M., Nishikawa, S., Yoshinaga, K., Hayashi, S., Kunisada, T., Nakao, J., Kina, T., Sudo, T. and Kodama, H. (1993). Expression and function of c-Kit in fetal hemopoietic progenitor cells: transition from the early c-Kit-independent to the late c-Kit-dependent wave of hemopoiesis in the murine embryo. *Development* **117**, 1089-1098.
Okuda, T., van Deursen, J., Hiebert, S. W., Grosveld, G. and Downing, J. R. (1996). AML1, the target of multiple chromosomal translocations in human leukemia, is essential for normal fetal liver hematopoiesis. *Cell* **84**, 321-330.
Osumi-Yamashita, N., Ninomiya, Y. and Eto, K. (1997). Mammalian craniofacial embryology in vitro. *Int. J. Dev. Biol.* **41**, 187-194.
Ottersbach, K. and Dzierzak, E. (2005). The murine placenta contains hematopoietic stem cells within the vascular labyrinth region. *Dev. Cell* **8**, 377-387.
Palis, J., Robertson, S., Kennedy, M., Wall, C. and Keller, G. (1999). Development of erythroid and myeloid progenitors in the yolk sac and embryo proper of the mouse. *Development* **126**, 5073-5084.
Peeters, M., Ottersbach, K., Bollerot, K., Orelio, C., de Bruijn, M., Wijgerde, M. and Dzierzak, E. (2009). Ventral embryonic tissues and Hedgehog proteins induce early AGM hematopoietic stem cell development. *Development* **136**, 2613-2621.
Rhodes, K. E., Gekas, C., Wang, Y., Lux, C. T., Francis, C. S., Chan, D. N., Conway, S., Orkin, S. H., Yoder, M. C. and Mikkola, H. K. (2008). The emergence of hematopoietic stem cells is initiated in the placental vasculature in the absence of circulation. *Cell Stem Cell* **2**, 252-263.
Robb, L., Lyons, I., Li, R., Hartley, L., Kontgen, F., Harvey, R. P., Metcalf, D. and Begley, C. G. (1995). Absence of yolk sac hematopoiesis from mice with a targeted disruption of the scl gene. *Proc. Natl. Acad. Sci. USA* **92**, 7075-7079.
Robin, C., Ottersbach, K., Durand, C., Peeters, M., Vanes, L., Tybulewicz, V. and Dzierzak, E. (2006). An unexpected role for IL-3 in the embryonic development of hematopoietic stem cells. *Dev. Cell* **11**, 171-180.

Robin, C., Bollerot, K., Mendes, S., Haak, E., Crisan, M., Cerisoli, F., Lauw, I., Kaimakis, P., Jorna, R., Vermeulen, M. et al. (2009). Human placenta is a potent hematopoietic niche containing hematopoietic stem and progenitor cells throughout development. *Cell Stem Cell* **5**, 385-395.
Samokhvalov, I. M., Samokhvalova, N. I. and Nishikawa, S. (2007). Cell tracing shows the contribution of the yolk sac to adult haematopoiesis. *Nature* **446**, 1056-1061.
Scholzen, T. and Gerdes, J. (2000). The Ki-67 protein: from the known and the unknown. *J. Cell Physiol.* **182**, 311-322.
Shivdasani, R. A., Mayer, E. L. and Orkin, S. H. (1995). Absence of blood formation in mice lacking the T-cell leukaemia oncoprotein tal-1/SCL. *Nature* **373**, 432-434.
Silva, J., Dasgupta, S., Wang, G., Krishnamurthy, K., Ritter, E. and Bieberich, E. (2006). Lipids isolated from bone induce the migration of human breast cancer cells. *J. Lipid Res.* **47**, 724-733.
Sugiyama, D. and Tsuji, K. (2006). Definitive hematopoiesis from endothelial cells in the mouse embryo; a simple guide. *Trends Cardiovasc. Med.* **16**, 45-49.
Sugiyama, D., Ogawa, M., Hirose, I., Jaffredo, T., Arai, K. and Tsuji, K. (2003). Erythropoiesis from acetyl LDL incorporating endothelial cells at the preliver stage. *Blood* **101**, 4733-4738.
Sugiyama, D., Arai, K. and Tsuji, K. (2005). Definitive hematopoiesis from acetyl LDL incorporating endothelial cells in the mouse embryo. *Stem Cells Dev.* **14**, 687-696.
Sugiyama, D., Ogawa, M., Nakao, K., Osumi, N., Nishikawa, S., Arai, K., Nakahata, T. and Tsuji, K. (2007). B cell potential can be obtained from pre-circulatory yolk sac, but with low frequency. *Dev. Biol.* **301**, 53-61.
Sugiyama, T., Kohara, H., Noda, M. and Nagasawa, T. (2006). Maintenance of the hematopoietic stem cell pool by CXCL12-CXCR4 chemokine signaling in bone marrow stromal cell niches. *Immunity* **25**, 977-988.
Tsai, F. Y., Keller, G., Kuo, F. C., Weiss, M., Chen, J., Rosenblatt, M., Alt, F. W. and Orkin, S. H. (1994). An early haematopoietic defect in mice lacking the transcription factor GATA-2. *Nature* **371**, 221-226.
Wang, Q., Stacy, T., Binder, M., Marin-Padilla, M., Sharpe, A. H. and Speck, N. A. (1996). Disruption of the Cbfa2 gene causes necrosis and hemorrhaging in the central nervous system and blocks definitive hematopoiesis. *Proc. Natl. Acad. Sci. USA* **93**, 3444-3449.
Watson, E. D. and Cross, J. C. (2005). Development of structures and transport functions in the mouse placenta. *Physiology (Bethesda)* **20**, 180-193.
Yoder, M. C., Hiatt, K., Dutt, P., Mukherjee, P., Bodine, D. M. and Orlic, D. (1997a). Characterization of definitive lymphohematopoietic stem cells in the day 9 murine yolk sac. *Immunity* **7**, 335-344.
Yoder, M. C., Hiatt, K. and Mukherjee, P. (1997b). In vivo repopulating hematopoietic stem cells are present in the murine yolk sac at day 9.0 postcoitus. *Proc. Natl. Acad. Sci. USA* **94**, 6776-6780.
Yuasa, H., Oike, Y., Iwama, A., Nishikata, I., Sugiyama, D., Perkins, A., Mucenski, M. L., Suda, T. and Morishita, K. (2005). Oncogenic transcription factor Evi1 regulates hematopoietic stem cell proliferation through GATA-2 expression. *EMBO J.* **24**, 1976-1987.
Zeigler, B. M., Sugiyama, D., Chen, M., Guo, Y., Downs, K. M. and Speck, N. A. (2006). The allantois and chorion, when isolated before circulation or chorio-allantoic fusion, have hematopoietic potential. *Development* **133**, 4183-4192.